

**RDU1603133**

CELLULOSE NANOCRYSTALS INCORPORATED WITH HYDROXYPROPYL  
METHYLCELLULOSE AS BIOCOMPOSITE SCAFFOLDS FOR BONE TISSUE  
ENGINEERING



FARAH HANANI ZULKIFLI

RESEARCH VOTE NO:  
RDU1603133

Faculty of Industrial Sciences and Technology  
Universiti Malaysia Pahang

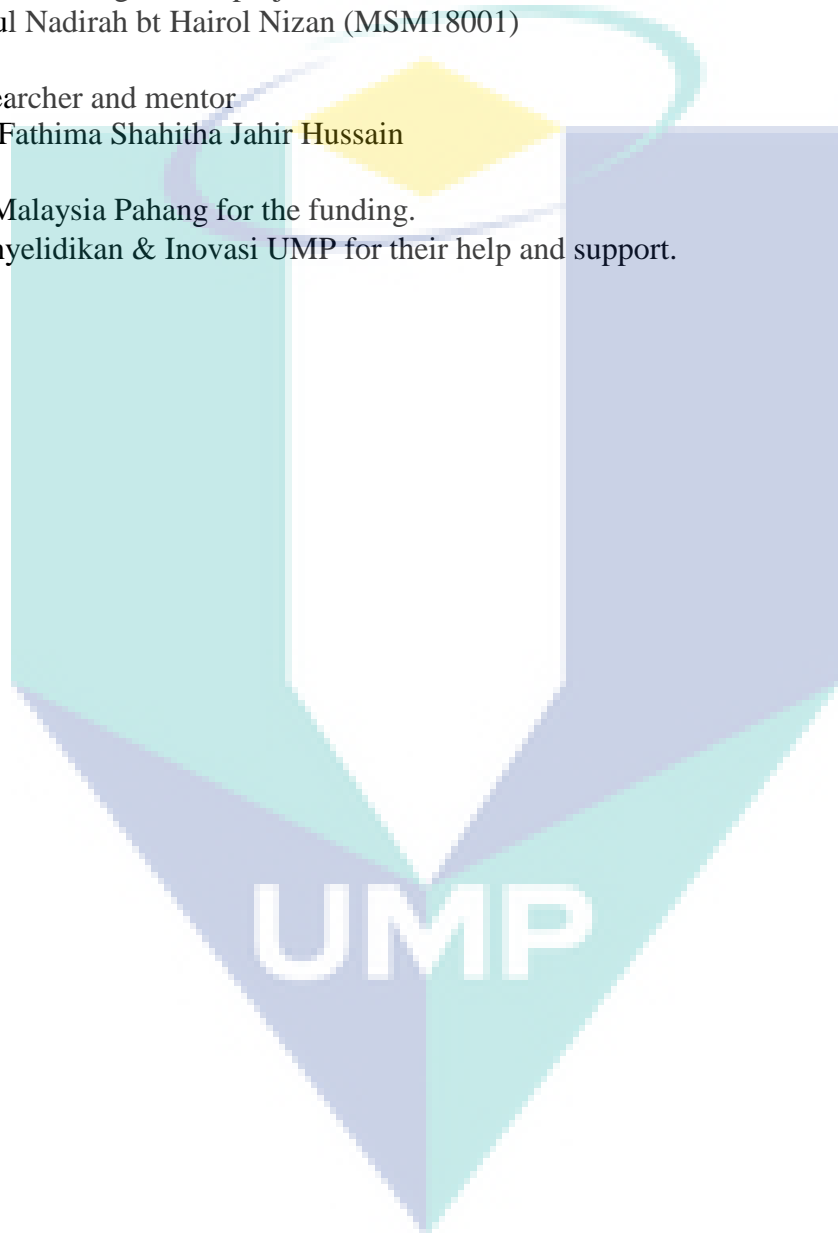
2019

UMP

## ACKNOWLEDGEMENT

I would like to thank the following people and organisations;

- The students working on this project  
Nor Sarahtul Nadirah bt Hairol Nizan (MSM18001)
- The co-researcher and mentor
  - Dr. Fathima Shahitha Jahir Hussain
- Universiti Malaysia Pahang for the funding.
- Jabatan Penyelidikan & Inovasi UMP for their help and support.



## Abstrak

### CELLULOSE NANOCRYSTALS INCORPORATED WITH HYDROXYPROPYL METHYLCELLULOSE AS BIOCOMPOSITE SCAFFOLDS FOR BONE TISSUE ENGINEERING

*(Keywords: hydroxypropyl methylcellulose, cellulose nanocrystals, bone tissue engineering)*

Dalam penyelidikan ini, tiga dimensi (3D) HPMC/PVA dan HPMC/PVA/CNC telah berjaya dihasilkan dengan menggunakan teknik pengeringan beku. HPMC (5 wt%) dan PVA (15 wt%) telah dilarutkan dan dicampur bersama pada nisbah 50:50 dan digabungkan dengan CNC (1, 3, 5, and 7 wt%) sebagai nanofiller untuk mendapatkan bahan yang mempunyai liang. Ciri-ciri morfologi, mekanikal dan terma dicirikan oleh SEM, ATR-FTIR, DSC dan TGA. Sementara itu, kajian sitotoksiti pada kedua-dua bahan dilakukan dengan menggunakan sel osteoblast janin manusia (hFOB) melalui ujian MTT dan DAPI pewarnaan. HPMC/PVA dengan CNC mempamerkan kefungsiannya yang lebih baik yang mengakibatkan penurunan saiz liang dan terdapat sedikit perubahan struktur kimia seperti yang ditentukan oleh spektrum FTIR. Kajian termal menunjukkan bahawa suhu lebur perancah HPMC/PVA/CNC beralih kepada nilai yang lebih tinggi. Sel-sel hFOB dapat melekat dan menyebarkan di kedua-dua perancah. Kajian juga mendapati ianya dapat menyokong perekatan sel dan percambahan sel. Oleh kerana ciri-ciri biokompatibel dan biodegradablenya, bahan yang baru ini boleh menghasilkan matriks perancah alternatif bagi menjanjikan pertumbuhan semula di dalam kejuruteraan tisu tulang.

The logo of Universiti Malaysia Perlis (UMP) is a large, stylized letter 'U' composed of several overlapping triangles in shades of blue and teal. The letters 'UMP' are printed in white, bold, sans-serif font across the center of the 'U'.

E-mail : [farahhanani@ump.edu.my](mailto:farahhanani@ump.edu.my)  
Tel. No. : +60162054397  
Vote No. : RDU1603133

## ABSTRACT

### CELLULOSE NANOCRYSTALS INCORPORATED WITH HYDROXYPROPYL METHYLCELLULOSE AS BIOCOMPOSITE SCAFFOLDS FOR BONE TISSUE ENGINEERING

*(Keywords: hydroxypropyl methylcellulose, cellulose nanocrystals, bone tissue engineering)*

In this present work, a porous three-dimensional (3D) scaffold of HPMC/PVA and HPMC/PVA/CNC were successfully fabricated by freeze-drying technique. HPMC (5 wt%) and PVA (15 wt%) were dissolved and blended at a ratio of 50:50 and incorporated with CNC (1, 3, 5 and 7 wt%) as nanofiller to obtain a highly porous scaffolds. The morphology, mechanical and thermal properties of scaffolds were characterized by SEM, ATR-FTIR, and TGA. Meanwhile, cytotoxicity studies on both porous scaffold biomaterials were carried out by utilizing human fetal osteoblast (hFOB) cells using MTT assays and DAPI staining. Incorporated HPMC/PVA with CNC were exhibited superior functionality which resulted in decreasing average pore size and there were slightly changes in the chemical structure as determined by FTIR spectra. Thermal studies revealed that the melting temperatures of HPMC/PVA/CNC scaffold were slightly shifted to a higher value. It was observed that the hFOB cells were able to attach and spread on both scaffolds and supported the cell adhesion and proliferation. Due to its biocompatible and biodegradable properties, these newly developed highly porous scaffolds may provide a promising alternative scaffolding matrix for bone tissue engineering regeneration.

The logo of Universiti Malaysia Perlis (UMP) is a large, stylized letter 'V' shape. The left side of the 'V' is light blue, the right side is light green, and the bottom point is a darker blue. The letters 'UMP' are written in white, bold, sans-serif font across the center of the 'V'.

E-mail : [farahhanani@ump.edu.my](mailto:farahhanani@ump.edu.my)

Tel. No. : +60162054397

Vote No. : RDU1603133

## TABLE OF CONTENT

<b>ABSTRAK</b>		<b>iii</b>
<b>ABSTRACT</b>		<b>iv</b>
<b>TABLE OF CONTENT</b>		<b>v</b>
<b>LIST OF TABLES</b>		<b>viii</b>
<b>LIST OF FIGURES</b>		<b>ix</b>
<b>LIST OF SYMBOLS/UNITS</b>		<b>xii</b>
<b>LIST OF ABBREVIATIONS</b>		<b>xiii</b>
<b>CHAPTER 1 INTRODUCTION</b>		
1.1	Background	1
1.2	Problem statement	3
1.3	Significance of studies	4
1.4	Research objectives	4
1.5	Research scope	5
1.6	Thesis outline	6
<b>CHAPTER 2 LITERATURE REVIEW</b>		
2.1	Human bone physiology	7
	2.1.1 General function of bone	8
	2.1.2 Structural and mechanical properties of bone	8
2.2	Bone tissue engineering	9
2.3	Biomaterials in tissue engineering	10
	2.3.1 Evolution of biomaterials	10
	2.3.2 Characteristics of biomaterials scaffold	11
	2.3.3 Hydroxypropyl methylcellulose (HPMC)	11
	2.3.4 Poly (vinyl) Alcohol (PVA)	12
	2.3.6 Cellulose nanocrystal (CNC)	12
2.4	Fabrication of scaffolds	13
	2.4.1 Freeze-drying technique	14

2.5	Summary	15
-----	---------	----

### **CHAPTER 3 METHODOLOGY**

3.1	Research methodology	16
3.2	Raw materials	19
3.3	Preparation of polymeric solution	19
3.4	Fabrication of porous material using freeze-drying method	20
3.5	Samples crosslinking	21
3.6	Characterization of CNC nanoparticle and HPMC/PVA/CNCs scaffolds	21
3.6.1	Field emission scanning electron microscope (FESEM)	22
3.6.2	Scanning electron microscope (SEM)	22
3.6.3	Porosity study	23
3.6.4	Attenuated total reflectance-Fourier Transform Infrared Spectroscopy (ATR- FTIR)	24
3.6.5	Thermogravimetric (TGA) analysis	24
3.6.6	Differential scanning calorimetry (DSC)	25
3.6.7	Mechanical testing	27
3.7	In vitro degradation study	28
3.7.1	Swelling ratio study	28
3.7.2	pH value measurements	29
3.7.3	Weight loss study	29
3.8	Cell culture study	29
3.8.1	In vitro cell culture study of HPMC/PVA/CNC scaffolds	30
3.8.2	hFOB cells expansion and seeding	30
3.8.3	hFOB cells morphology studies	32
3.8.4	hFOB cells proliferation study	32

### **CHAPTER 4 RESULTS AND DISCUSSION**

4.1	Characterization of CNC	35
4.1.1	Morphology of CNC	35
4.1.2	Chemical properties of CNC	36
4.1.3	Thermal study of CNC	36
4.2	Characterization of HPMC/PVA and HPMC/PVA/CNCs scaffolds	37
4.2.1	Morphology of scaffolds	38
4.2.2	Porosity	40
4.2.3	ATR-FTIR study	41
4.2.4	TGA measurements	42

4.2.5	DSC study	44
4.2.6	Mechanical properties	45
4.3	In vitro degradation study of HPMC/PVA and HPMC/PVA/CNCs scaffolds	46
4.3.1	Weight loss, swelling ratio and pH value analysis	47
4.4	Cell culture studies on HPMC/PVA and HPMC/PVA/CNCs for bone tissue engineering applications	48
4.4.1	hFOB cells proliferation on scaffolds	48
4.4.2	hFOB cells morphology studies on scaffolds	51
<b>CHAPTER 5 CONCLUSION</b>		
5.1	Summary	55
5.2	Recommendations for future studies	55
<b>REFERENCES</b>		<b>56</b>

The logo for UIMP (Universiti Malaysia Perlis) is a large, stylized shield shape. It is composed of several overlapping geometric shapes in shades of teal, light blue, and yellow. The letters 'UIMP' are written in a bold, white, sans-serif font across the bottom center of the shield.

UIMP

**LIST OF TABLES**

<b>Table No.</b>	<b>Title</b>	<b>Page</b>
2.1	Past research projects used freeze-drying method	14
3.1	Composition of CNCs in HPMC/PVA blended polymer	20
4.1	TGA and DTA for all scaffolds	44
4.2	Compressive strength and Young's modulus for all scaffolds	46



**UMP**

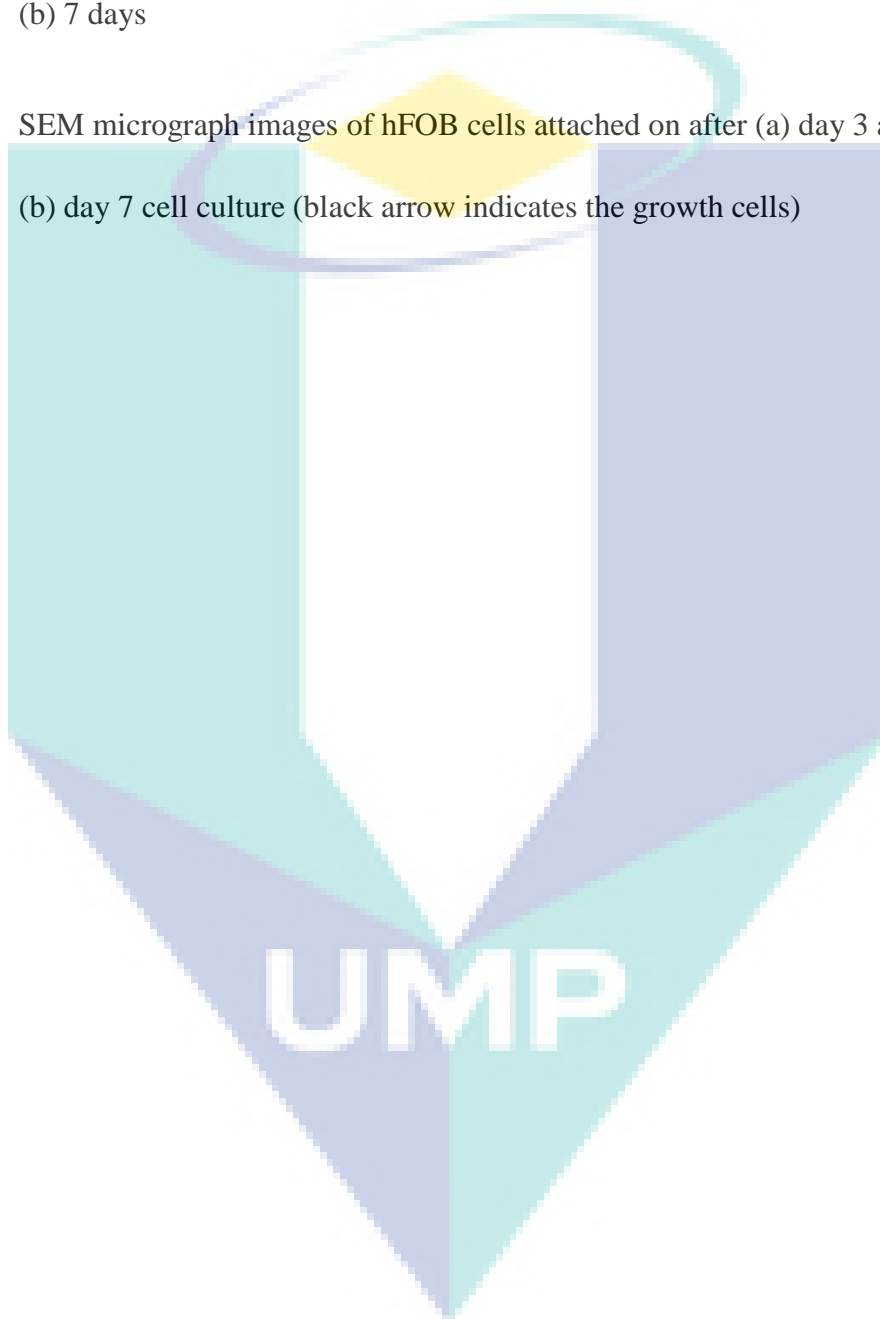


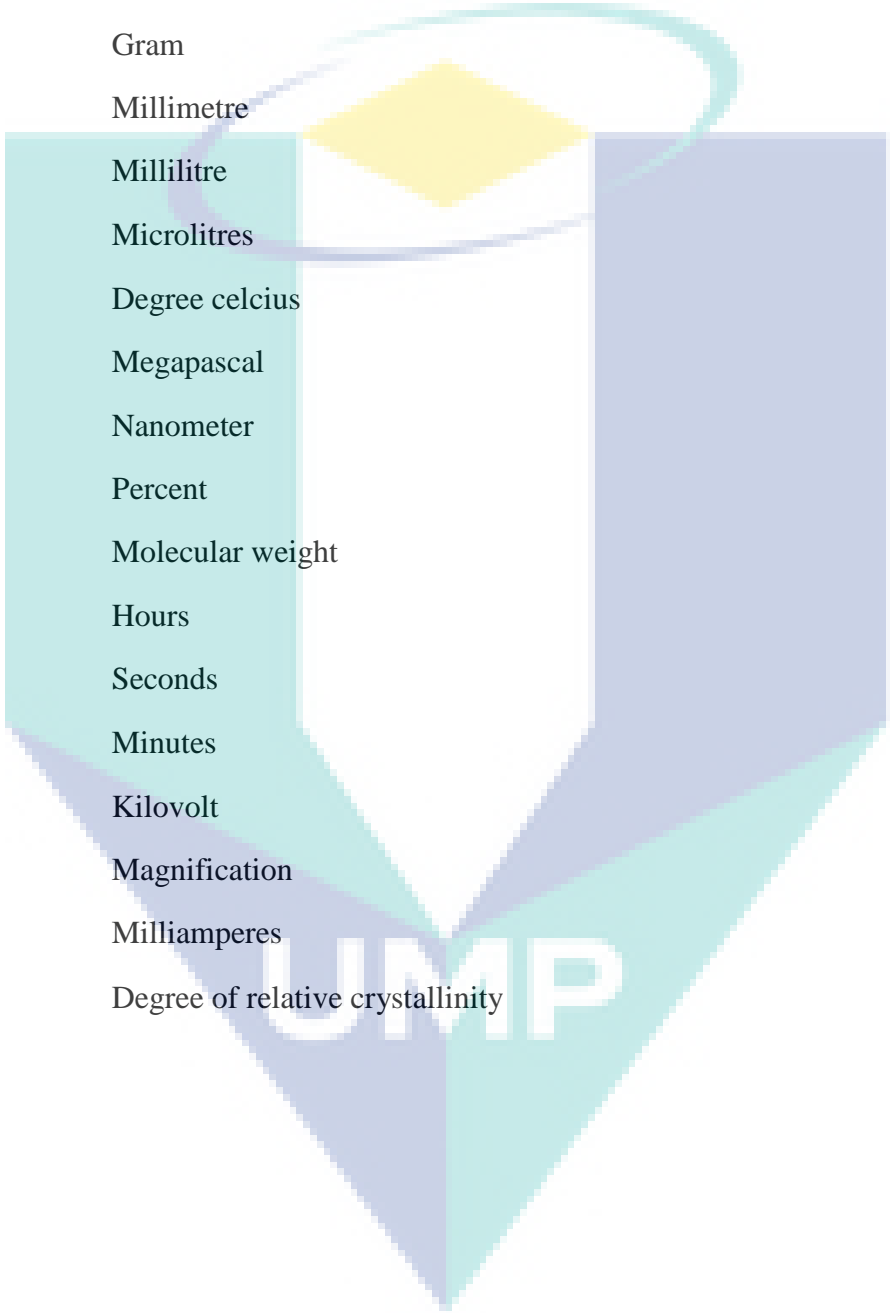
## LIST OF FIGURES

Figure No.	Title	Page
2.1	Bone anatomy cortex: (i) Cancellous bone and (ii) Cortical bone	9
2.2	Molecular structure of HPMC 11	
2.3	Chemical structure of cellulose	13
3.1	Summary of research methodology implemented in this research	17
3.2	Flowchart of research methodology implemented in this research	18
3.3	Cellulose	19
3.4	Photograph of freeze-dryer machine, Labconco	21
3.5	Photograph of FESEM, JSM-7800F Extreme-resolution Analytical	22
3.6	Photograph of SEM, FEI QUANTA 450	23
3.7	Photograph of ATR-FTIR, Perkin-Elmer.	24
3.8	Photograph of TGA, Q500.	25
3.9	Photographs of DSC, NETZSCH	26
3.10	DSC thermograms	27
3.11	Photograph of universal testing machine, Shimadzu	28
3.12	Photograph of Horiba LAQUA Handheld Water Quality Analysis Meters	29
3.13	Summarize of cell culture study	30
3.14	hFOB cell in cell culture flask	31
3.15	Cell culture studies of scaffolds at different weight ratios	32
3.16	Photograph of EVOS inverted microscope	33
3.17	Photograph of NanoQuant micro plate reader (infinite M200PRO)	34

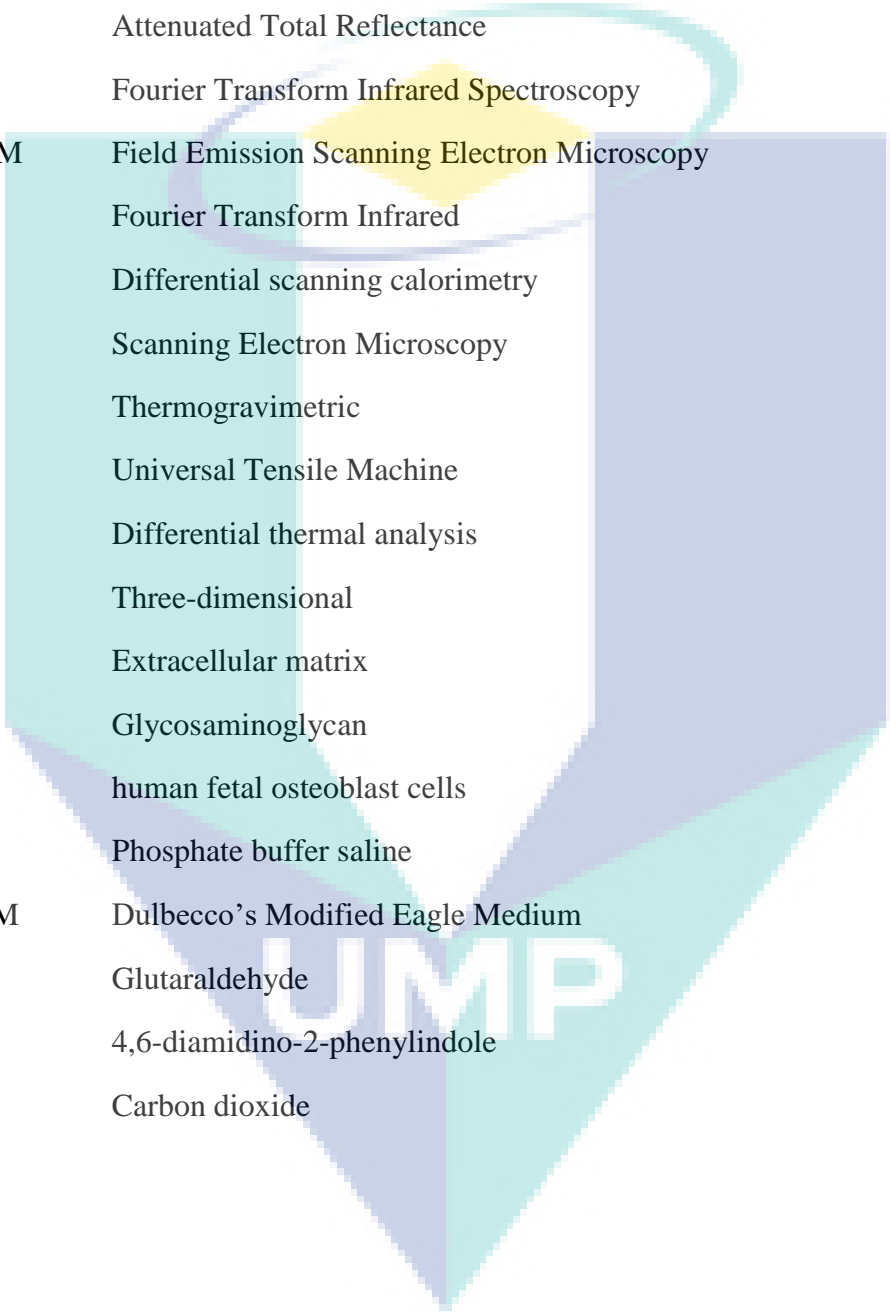
4.1	FESEM micrographs of CNC nanocrystals at 50 000×	35
4.2	ATR-FTIR analysis of CNC nanocrystals	36
4.3	DSC thermograms of CNC nanocrystals	37
4.4	HPMC/PVA and HPMC/PVA/CNC (1, 3, 5, 7 wt%) polymeric solutions	37
4.5	HPMC/PVA and HPMC/PVA/CNC (1,3,5,7 wt%) scaffolds	38
4.6	SEM micrographs of HPMC/PVA interconnected porous scaffolds with different CNC concentration at (1,3,5 and 7 wt%)	39
4.7	Porosity of CNC, HPMC and PVA alone and HPMC/PVA scaffolds with different CNC concentration at (1,3,5 and 7 wt%)	40
4.8	ATR-FTIR spectra of CNC, HPMC and PVA alone and HPMC/PVA scaffolds with different CNC concentration at (1,3,5 and 7 wt%)	42
4.9	TGA and DTA curves for HPMC/PVA scaffolds with different CNC concentration at (1,3,5 and 7 wt%)	43
4.10	DSC thermograms of CNC, HPMC and PVA alone and HPMC/PVA scaffolds with different CNC concentration at (1,3,5 and 7 wt%)	44
4.11	Compressive strength for HPMC/PVA scaffolds with different CNC concentration at (1,3,5 and 7 wt%)	45
4.12	Weight loss for HPMC/PVA scaffolds with different CNC concentration at (1,3,5 and 7 wt%)	47
4.13	pH value analysis of HPMC/PVA and HPMC/PVA/CNC (1, 3, 5, 7 wt%) porous scaffolds	48

- 4.14 Graph showing human osteoblast viability after 1, 3, 5 and 7 days of incubation( $1 \times 10^5$  cells/well in complete DMEM) at different weight ratios of scaffolds 49
- 4.15 DAPI stained osteoblast cells grown in scaffolds at (a) 3 days and (b) 7 days 50
- 4.16 SEM micrograph images of hFOB cells attached on after (a) day 3 and (b) day 7 cell culture (black arrow indicates the growth cells) 52



**LIST OF SYMBOLS/UNITS**

cm	Centimetres
wt	Weight percent
g	Gram
mm	Millimetre
mL	Millilitre
$\mu\text{L}$	Microlitres
$^{\circ}\text{C}$	Degree celcius
MPa	Megapascal
nm	Nanometer
%	Percent
$M_w$	Molecular weight
h	Hours
s	Seconds
min	Minutes
kV	Kilovolt
x	Magnification
mA	Milliamperes
$\chi_c$	Degree of relative crystallinity

**LIST OF ABBREVIATIONS**

HPMC	Hydroxethyl cellulose
PVA	Poly (vinyl alcohol)
CNC	Cellulose nanocrystal
ATR	Attenuated Total Reflectance
FTIR	Fourier Transform Infrared Spectroscopy
FESEM	Field Emission Scanning Electron Microscopy
FTIR	Fourier Transform Infrared
DSC	Differential scanning calorimetry
SEM	Scanning Electron Microscopy
TGA	Thermogravimetric
UTM	Universal Tensile Machine
DTA	Differential thermal analysis
3D	Three-dimensional
ECM	Extracellular matrix
GAG	Glycosaminoglycan
hFOB	human fetal osteoblast cells
PBS	Phosphate buffer saline
DMEM	Dulbecco's Modified Eagle Medium
GA	Glutaraldehyde
DAPI	4,6-diamidino-2-phenylindole
CO <sub>2</sub>	Carbon dioxide



## CHAPTER 1

### INTRODUCTION

#### 1.1 Background

The emergence field of tissue engineering has substantially revolutionized the functionalization of biomaterials, thus overcome the limitation of traditional tissue transplantation (Bhat & Kumar, 2013). Generally, tissue and organ transplantations represent accepted therapies, but they are dramatically limited by donor shortages (Caló & Khutoryanskiy, 2015). Tissue engineering or regenerative medicine promises to solve problems in organ transplantation by utilized the application of chemical, biological and engineering principles to replace or repair the damaged or effected living tissues like bone, cartilage and skin using biomaterials, cells, and growth factors, alone or in combination. The strategies are categorized into three groups which are direct injection of cells into the tissue of interest, implantation of cell-scaffold constructs (3D tissue structure), and scaffold-based delivery of drugs and/or signaling molecules such as growth factors to stimulate cell growth, migration, and differentiation (Kumar et al., 2016).

Next, the most critical factor to be considered in tissue engineering is the interaction of cells with ideal scaffolds, which serve to be the template in order to promote growth of the tissue. Scaffold can be described as a temporary substrate to support the neovascularization and propagation of cells at the defects area of living tissue. In bone tissue engineering, scaffold plays an important role in manipulating the

functions of osteoblasts and acts as central role to guide new bone formation into desired shapes (Saber-Samandari, Saber-Samandari, Kiyazar, Aghazadeh, & Sadeghi, 2016). Scaffolds that are being placed and introduced at the defective site should mimic the artificial extracellular matrix (ECM) of human body (Hirano & Mooney, 2004). ECM consists of fibrous collagen and proteoglycans. Proteoglycans are made of proteins and polysaccharide chains known as glycosaminoglycan (GAG). The interaction between the cells and the ECM is very important in biological systems. An ideal scaffold should biodegrade as the native tissue integrates and actively promote desirable physiological responses. Besides, an excellent scaffold should possess porous architecture, produce non-toxic degradation product and should be capable of sterilization without loss of bioactivity and should deliver bioactive molecules in a controlled fashion to accelerate healing. Hence, a suitable material scaffold is very important in all the strategies to engineer tissues.

Biomaterial is known to be a biological or synthetic substance which can be introduced into body tissue to replace or repair damaged tissue. Many natural and synthetic polymers were used as scaffolds due to its biocompatibility and biodegradability. Although there is wide range of biomaterials being fabricated and used as scaffolds, there is only few biopolymers that closely mimic to ECM by having polysaccharide chains in them. The most commonly biopolymer with chemical structure similar to GAGs in ECM is chitosan, which is a biocompatible and widely used in wound healing application (Kousaku Ohkawa, 2004). Other than that, cellulose which can be derived from natural resources such as plant, animal, or mineral plants has the potential to be used in various applications like sensor, biomedical and pharmaceutical and in packaging industries (Edwards, Prevost, Sethumadhavan, Ullah, & Condon, 2013).

Hydroxethyl cellulose (HPMC) is a non-ionic with  $\beta$  (1 $\rightarrow$ 4) glycosidic linkage held together with H-bonds. It is a biocompatible water soluble polysaccharide material with protective colloidal action. It is less expensive and commonly used in various pharmaceutical compositions, wound dressing and wound healing applications (H. Zhang, Nie, Li, White, & Zhu, 2009). In this study, HPMC will be mixed with poly (vinyl alcohol) (PVA), a polyhydroxy water soluble polymer. It is biocompatible and biodegradable and widely used in biomedical applications which include drug delivery

reservoirs, resorbable surgical sponges and many more. Combination of HPMC with other hydrogel like PVA improves the mechanical properties such as elasticity and elongation (Zulkifli, Hussain, Rasad, & Mohd Yusoff, 2014).

Cellulose nanocrystals (CNCs) have lots of advantages over other nanoparticles such as high surface area, high, non-toxicity, biodegradability and other optical properties. In general studies, CNCs are used to improve various mechanical and barrier properties of various biopolymers (Borkotoky, Dhar, & Katiyar, 2018).

The aim of this research is to elucidate the properties of HPMC/PVA scaffolds which incorporated with various concentrations of CNCs produced by freeze-drying technique and its potential as a substrate in bone tissue engineering. According to literature review, HPMC/PVA/CNC porous scaffolds have gained less attention as no reliable evidence about the development, which gave us the motivation to carry out this study. Herein, the physical and chemical interactions, and mechanical and thermal properties of scaffolds were characterized by SEM, ATR-FTIR, TGA, DSC and mechanical testing. Besides that, in vitro degradation and cell culture studies were carried out to investigate the biocompatibility of cell-scaffolds as this research was focusing on the bone tissue engineering application.

## **1.2 Problem statement**

The aging population and the increasing numbers of patients suffering from bone defects due to accidents or trauma leads to tremendous demand for bone substitute. The traditional methods that had been introduced since many years ago which are autografts and allografts being used to treat burns or other full thickness skin defects. Autografts have a higher success rate but are limited in supply and may cause donor site morbidity where allografts have always given risk for disease transmission and immunological rejection. Nowadays, scientists and researchers were constantly and continually developing method to overcome the problem arises in traditional methods.

Thus, tissue engineering has emerged as a promising alternative to treat injuries involves scaffolds, cells and biological cues alone or in combination (MacNeil, 2007). In tissue engineering, scaffolds, on which tissue was grown is one of the fundamental structures to be optimized for desired bone implant. Although bone tissue engineering



has been the issue of considerable research in the era of regenerative medicine over the past two decades, many skeletal problems stay undertreated. These might be due to the current high cost of scaffolding technique, incompatible with native tissues, toxicity, and unmatched biodegradable healing periods. For that reason, the requirement for reliable, humane, and ecofriendly scaffold must be given attention in order to investigate a biomimetic scaffolds that not only possess biocompatible, biodegradable, non-toxic and neovascularization properties, but also cost-effective and shelf presented. Besides, although intensive studies have been done to find an alternative bone implants, the commercialization of this product is yet to be reached. Due to that motivation, a depth study to develop a new combination of biopolymeric materials is crucial yet favorable, so that the gap between the demand and the lack of supply of orthopedic products could be filled.

### **1.3 Significance of studies**

In this work, HPMC/PVA/CNCs polymeric solutions were prepared using deionized water as the only solvent, fabricated using freeze-drying technique and cross linked via heat treatment. This research aims to develop non-toxic, biocompatible, and biodegradable scaffolds since the demands on economical, safe and rapid-healing process of implant tissues or organs are intensely increased by year. It is worth to mention that CNC have garnered a tremendous level of attention in material community due to its unique features. The outcomes of this study may contribute to the medical community especially those who work in bone tissue engineering as well as low and middle-class patients who suffered from bone injuries or defects that prerequisite cost-effective scaffolds with rapid healing response. To the best of our knowledge, this is the first study on the effect of concentration of CNCs in HPMC/PVA porous scaffolds, characterized, and applied in the bone tissue engineering application. This research may give contribution to the development of tissue engineering products in healthcare industry.

### **1.4 Research objective**

The objectives of this research are:

1. To fabricate HPMC/PVA porous scaffolds incorporated with CNCs as nanofillers using freeze-drying technique.
2. To study the effect of various concentrations of CNCs in HPMC/PVA scaffolds based on the physical and chemical interaction, thermal and mechanical properties.
3. To investigate the biocompatibility of HPMC/PVA/CNC scaffolds as a potential substrate for bone tissue engineering application.

### **1.5 Research scope**

The following research scopes are essential to achieve the first objective:

- i. To observe the image of CNC using FESEM and measure its dimensions by using imageJ software.
- ii. To identify the functional groups of CNC using ATR-FTIR spectra.
- iii. To study the thermal stability of CNC using DSC

The following research scopes are necessary to achieve the second objective:

- i. To observe the surface morphology of all scaffolds via SEM images and measure the pore size by ImageJ software.
- ii. To identify the functional groups of all scaffolds using ATR-FTIR spectra.
- iii. To study the thermal stability and decomposition behavior of scaffolds using TGA and DSC.
- iv. To study the mechanical strength of scaffolds by analyzing the stress-strain curves using UTM.
- v. To investigate the degradation behavior of porous scaffolds in PBS at different time points. The analysis will involve pH changes of the solution, weight loss and swelling ratio.

Finally, the following research scopes are necessary to achieve the third objective:

- i. To investigate the cellular biocompatibility by carrying out in vitro cell culture studies using human fetal osteoblast (hFOB) cell.
- ii. To determine the adherence, differentiation and proliferation of hFOB cells on the scaffolds using DAPI staining and MTT assays by measuring the absorbance value and observe the surface morphology changes by SEM.
- iii. To identify the optimum concentration of CNCs in HPMC/PVA scaffolds that display better responsive towards hFOB cells.

## **1.6 Research outline**

The following is a brief outline regarding the contents of this thesis. Chapter 2 provides a comprehensive overview on related topics to this study including recent research on bone tissue engineering and details of polymeric materials involved in this project. In Chapter 3, the research methodology will presents the materials used and experimental method applied in this research. The working principle of each instruments used for characterization will be also stated. Next, Chapter 4 will be discussed the synthesis and characterization of all scaffolds including the cell culture studies for bone tissue engineering application. Finally, in Chapter 5, the summary of this research and the recommendations for future reference will be discussed.

## CHAPTER 2

### LITERATURE REVIEW

#### 2.1 Human bone physiology

Bone is a special form of connective tissue, which unlike most other tissues is physiologically mineralized. On the organ level, bone is made up of the cartilaginous joints, the calcified cartilage of the growth plate (during skeletal growth only), the marrow space, and the mineralized cortical and trabecular bone structures (Kneissel, 2017). The four general categories of bones are long bones, short bones, flat bones, and irregular bones. Long bones include the clavicles, humeri, radii, ulnae, metacarpals, femurs, tibiae, fibulae, metatarsals, and phalanges. Short bones include the carpal and tarsal bones, patellae, and sesamoid bones. Flat bones include the skull, mandible, scapulae, sternum, and ribs. Irregular bones include the vertebrae, sacrum, coccyx, and hyoid bone. Flat bones form by membranous bone formation, whereas long bones are formed by a combination of endochondral and membranous bone formation (Clarke, 2008).

On the tissue level, bone consists of the mineralized and non-mineralized matrix (osteoid) and the three principal cellular components, the bone-forming osteoblasts, some of which become entrapped into the mineralizing bone matrix they lay down to become osteocytes, and the bone-resorbing osteoclasts. The origin of these cell types as well as the communication between them and their involvement in vital processes such as skeletal growth, bone adaptation (modeling) and bone maintenance (remodeling).

On the organ level, based on their anatomical location, bones can be divided into four distinct envelopes, namely, subperiosteal, endocortical, cancellous, and

intracortical. They play different roles in bone biology in health and disease and differ in their response to changes in the mechanical environment.

### **2.1.1 General function of bone**

Bone is a multifunctional tissue which serves as mechanical support and protection, is an essential part of hematopoiesis and mineral metabolism, and has a role as an endocrine organ. Bone is able to resist deformation from impact loading, but at the same time, it is also able to absorb or dissipate energy by changing shape without cracking. The elastic properties of bone allow it to absorb energy by deforming reversibly when loaded. As a rigid organ in body, the bone is able to support and protect various organs but is also able to facilitate mobility

### **2.1.2 Structural and mechanical properties of bone**

The adult human skeleton has a total of 213 bones, excluding the sesamoid bones. The appendicular skeleton has 126 bones, axial skeleton 74 bones, and auditory ossicles 6 bones. Each bone constantly undergoes modeling during life to help it adapt to changing biomechanical forces, as well as remodeling to remove old, microdamaged bone and replace it with new, mechanically stronger bone to help preserve bone strength (Clarke, 2008).

Figure 2.1 shows the bone anatomy cortex. Human bone is classified by a compressive strength where the (i) cancellous bone is ~7–10 MPa and for the (ii) cortical bone is ~170–193 MPa, respectively (Kumar et al., 2016). Therefore, to ensure the stability of implant, it is crucial to have a biomaterial with mechanical properties that is more or less similar to the bone.

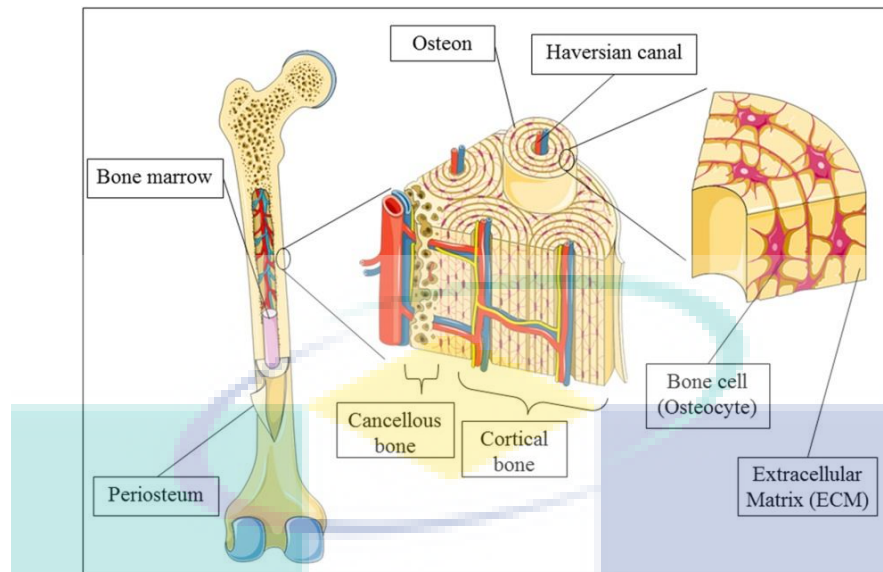


Figure 2.1 Bone anatomy cortex: (i) Cancellous bone and (ii) Cortical bone.

## 2.2 Bone tissue engineering

Bone is a vascularized connective tissue that supports and protects various internal organs of the body, produce red and white blood cells and enable mobility. Unlike many other tissues in the body, bones possess the property of regeneration and remodeling in response to injury. Bone remodeling is influenced by the calcium levels in the blood and the pull of muscles on bone (Preethi Soundarya, Sanjay, Haritha Menon, Dhivya, & Selvamurugan, 2018). Primary bone is defined as new bone formed in a space where previously no bone existed, or formed on an existing surface of bone or mineralized cartilage. Thus, primary bone requires only bone formation, whereas secondary bone is defined as bone which is produced by the resorption of previously deposited bone followed by the formation of new bone in its place, a process called remodelling.

Bone tissue engineering involves the improvement or replacement of specific tissues or organs using engineered materials and synthetic strategies (Caló & Khutoryanskiy, 2015). From the literature review, it is reported that there are millions of patients suffering from the loss or failure of an organ or a tissue caused by an accident or a disease every year. Over 8 million surgeries are conducted to treat these patients in the U.S. each year, and the overall cost of these issues to the U.S. economy is estimated to be around \$400 billion per year. With increasing numbers of bone

injuries cases reported, tissue engineers face one of the biggest challenges in order to come out with a new and advance invention with low cost consuming. Solutions to these problems will significantly advance tissue engineering and regenerative medicine.

### **2.3 Biomaterials in tissue engineering**

Biomaterial can be classified into two categories; (i) natural and (ii) synthetic polymers. Natural polymers suffer from some disadvantages and due to that, synthetic polymers are preferred over natural polymers (Gavasane, 2014). The synthetic polymers are categorized into biodegradable and non-biodegradable polymers. The selection of a polymer is a challenging task because of the inherent diversity of structures and thus it requires a thorough understanding of the surface and bulk properties of the polymer that can give the desired chemical, interfacial, mechanical and biological functions. Biodegradable polymers are currently being investigated as drug delivery systems or as scaffolds for tissue engineering. Polymers possess a unique strength in tissue engineering which enables the new advancement in human bone system which improves the therapy and treatment. Biodegradable polymers have proven their potential for the development of new, advanced and efficient in this field (Gavasane, 2014).

#### **2.3.1 Evolution of biomaterials**

Previously, osteoporosis caused by either trauma or diseases which are categorized as the bone fractures and skeletal disorders are traditionally treated by reconstructed the bone using permanent or/and temporary implant which involve the usage of titanium, alloys and stainless steel. The mechanical properties and materials of implants must be suitable for long term performance under physiological condition. Nowadays, composite materials (i.e., ceramics and polymers) are better choices as bone tissue engineering scaffolds, since natural bone matrix is an organic/inorganic composite material. Composite materials often show an excellent balance between strength and toughness, and usually have characteristics that are improvements on those of their individual components. Besides having enough mechanical strength to provide structural support, the scaffold's material must be biocompatible and osteoconductive. Materials that have been documented and used most often in scaffold fabrication include sodium alginate, chitosan, cellulose, chitosan/hydroxyapatite, chitosan/alginate,

hydroxyapatite, collagen/hydroxyapatite, and polyacrylamide/ hydroxyapatite (Saber-Samandari et al., 2016).

### 2.3.2 Characteristics of biomaterials scaffold

The use of biodegradable polymers as scaffolds on which layers of cells are grown is an alternate tissue-engineering approach for the development of a functional bone tissue. The scaffold degrades and is replaced and remodeled by the ECM secreted by the cells. An alternative strategy to synthetic and degradable scaffold is the manipulation of proteins that constitute the architecture of native ECM. Ultimately, the success of this approach is dependent on appropriate cell migration, adhesion and proliferation, as well as ECM production, on the biomimetic surfaces.

### 2.3.3 Hydroxypropyl methylcellulose (HPMC)

HPMC is a white or light yellow fibrous or powdery solid, tasteless and nontoxic, prepared from the alkaline cellulose and ethylene oxide (or chlorine ethanol) by etherification, and belongs to non-ionic soluble cellulose ethers. HPMC is a non-ionic hydrophilic polysaccharides biopolymers with  $\beta(1\rightarrow4)$  glycosidic linkage. HPMC groups attach to the OH groups of the polysaccharide structure by ether linkages as shown in Figure 2.2. This hydrogel functions as a stabilizing and protective colloid. HPMC is widely used in cosmetic, pharmaceutical and wound healing applications. It is well known that these types of hydrogels with large amount of water diffused in three dimensional polymeric networks are highly needed in biomedical and health applications. Cross-linking these hydrogels by various chemical bonds and physical interactions can significantly improve their mechanical, thermal and chemical properties.

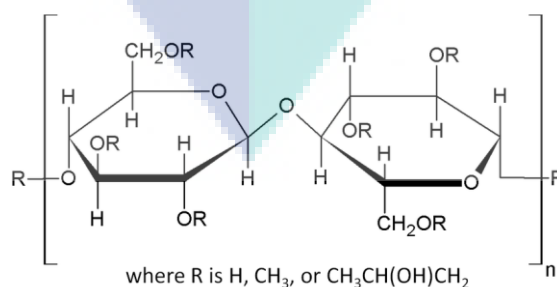


Figure 2.2 Molecular structure of HPMC



### 2.3.4 Poly (vinyl alcohol) (PVA)

Poly (vinyl alcohol) (PVA) has excellent film- and fiber-forming, emulsifying, surfactant and adhesive properties. It is also utilized to fabricate unique porous scaffolds composition matrix polymers. PVA is odorless and nontoxic, and has high tensile strength and flexibility, as well as high oxygen and aroma barrier properties. All of these properties ultimately depend on the humidity of PVA (with higher humidity more water is absorbed). The water, which acts as a plasticizer, will reduce tensile strength, but increase the material's elongation and tear strength. PVA has a melting point of 230 °C and 180 and 190 °C for the fully hydrolyzed and partially hydrolyzed grades, respectively. PVA decomposes rapidly above 200 °C as it can undergo pyrolysis at high temperatures (Gokmen et al., 2015).

### 2.3.5 Cellulose nanocrystal (CNC)

Cellulose is the world's most abundant renewable polymer resource and has been used as an engineering material for thousands of years. By extracting cellulose at the nanoscale, the majority of the defects associated with its hierarchical structure can be removed, and a new generation of material–cellulose nanoparticles can be obtained, which is an ideal material to base the new biopolymer nanocomposite industry. The preparation of reinforced polymer materials with cellulose nanoparticles has seen rapid advances and considerable interest in the last decade owing to its renewable nature, high mechanical properties, and low density, as well as its availability and the diversity of its sources.

Cellulose nanocrystals (CNCs) are defect-free, rod-like crystalline residues obtained when cellulose is subjected to acid hydrolysis from wide variety of natural sources such as wood, grass stalks, bacteria and alga. CNCs have attracted great attention due to their high aspect ratio (3 to 5 nm wide, 50 to 500 nm in length) and high crystallinity (54 to 88%) (C. Zhang et al., 2015)

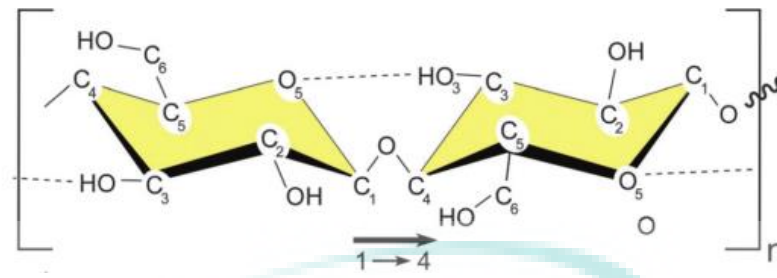


Figure 2.3 Chemical structure of cellulose

## 2.4 Fabrication of scaffolds

The fabrication of continuous ultrafine fibers of various polymers that could mimic the natural ECM structure has been extensively explored for decades. Preparation of porous scaffolds involved some methods such as gas-forming foam, three-dimensional printing, solvent casting/particulate leaching, thermal-induced phase separation, freeze-drying and electrospinning (Saber-Samandari et al., 2016).

UMP

Table 2.1 Past research projects used freeze-drying method

Research journal	Sample form	Reference
Processing and characterization of chitosan/PVA and methylcellulose porous scaffolds for tissue engineering	CS/PVA/MC porous scaffold	(Kanimozhi, Basha, & Sugantha Kumari, 2016)
Effects of molding temperature, pressure and time on polyvinyl alcohol nanocomposites properties produced by freeze drying technique	PVA/CNF nanocomposite films	(Salehpour, Jonoobi, & Rafieian, Oksman, 2018)
Fabrication and characterization of nanobiocomposite scaffold of zein/chitosan/nanohydroxyapatite prepared by freeze-drying method for bone tissue engineering	ZN/CS/nHAp composite scaffolds	(Shahbazarab, Teimouri, Chermahini, & Azadi, 2018)
Biomaterials based on freeze dried surface-deacetylated chitin nanofibers reinforced with sulfobutyl ether $\beta$ -cyclodextrin gel in wound dressing applications	SDACNFs/SBE- $\beta$ -CD scaffolds	(Tabuchi et al., 2016)
Morphology and properties of poly vinyl alcohol (PVA) scaffolds: Impact of process variables	PVA scaffolds	(Ye, Mohanty, & Ghosh, 2014)
Development of poly(vinyl alcohol) porous scaffold with high strength and well ciprofloxacin release efficiency	PVA/PEG/Cip porous scaffold	(Zhou et al., 2016)

In tissue engineering, highly porous scaffolds produced by freeze-drying technique is highly favorable and has demonstrated the most promising results for cell adhesion, proliferation and differentiation for regenerative medicine applications. Table 2.1 above summarized some of the research that has been done using freeze-drying method to get scaffold.

#### 2.4.1 Freeze-drying technique

Freeze drying can be describe as the technique used to improve the physical and chemical stability of colloidal nanoparticles by removal of water from the aqueous

dispersionsto obtain them in a dried form (Ali & Lamprecht, 2017). The lyophilization of polymeric nanoparticles or freeze drying is frequently based in empirical principles, without considering the physical-chemical properties of formulations and the engineering principles of lyophilization. Therefore, the optimization of formulations and the lyophilization cycle is crucial to obtain a good lyophilizate, and guarantee the preservation of nanoparticles (Fonte, Reis, & Sarmiento, 2016).

## 2.5 Summary

To summarize, an amount of research has been undertaken to find the ideal scaffolds for bone tissue engineering applications. Although many products are commercially available in the market, there are still limitations in several criteria such as high costs, history of unsuccessful treatments, weak tensile properties, toxicity and instability during storage. In addition, most biomaterial polymers are found to dissolve the polymers. Regular or high exposures to organic solvents may induce environmental contamination as well as toxicity and general hazards to the workers.

This research aims to fabricate HPMC/PVA/CNC using deionized water as the only solvent and then investigate their potential as scaffolds in bone tissue engineering applications. By using extremely simple methods which is freeze drying, scaffolds produced via a 'green' environmentally friendly approach are easy and capable of processing in a large scale. To the best of our knowledge, this is the first report where CNC is synthesized and then followed by fabrication of HPMC/PVA/CNCs scaffolds via freeze-drying methods. All the characterization will be studied based on the application in bone tissue regeneration. In this study, CNC nanoparticle is chosen as additive polymers due to their biocompatibility, biodegradability and non-toxicity properties that offer better cell adherence, differentiation and proliferation on the scaffold's surfaces. All scaffolds will undergo an in vitro cell culture study by using human fetal osteoblast cells.

## CHAPTER 3

### METHODOLOGY

#### 3.1 Research methodology

This chapter discussed clearly about the whole process of the research. All materials and methods that have been applied in this research were explained in details starting with research methodology including the flow chart of this research, until the fabrication and characterizations of porous scaffolds and the procedures involved in the cell-culture experiment.

Figure 3.1 shows the summary of the research methodology implemented while flow chart in Figure 3.2 clarifies specifically about all works being done throughout this research. Freeze-drying method was conducted in order to obtain a highly porous scaffold. Firstly, the aqueous polymeric solutions of HPMC, PVA with various concentrations of CNCs were prepared by dissolving all the solutions in deionized water until obtained a homogenous solution. Then, the porous freeze-dried scaffolds were characterized based on their physical, chemical, thermal and mechanical properties. Finally, cell culture studies were carried out to observe the cell compatibility.

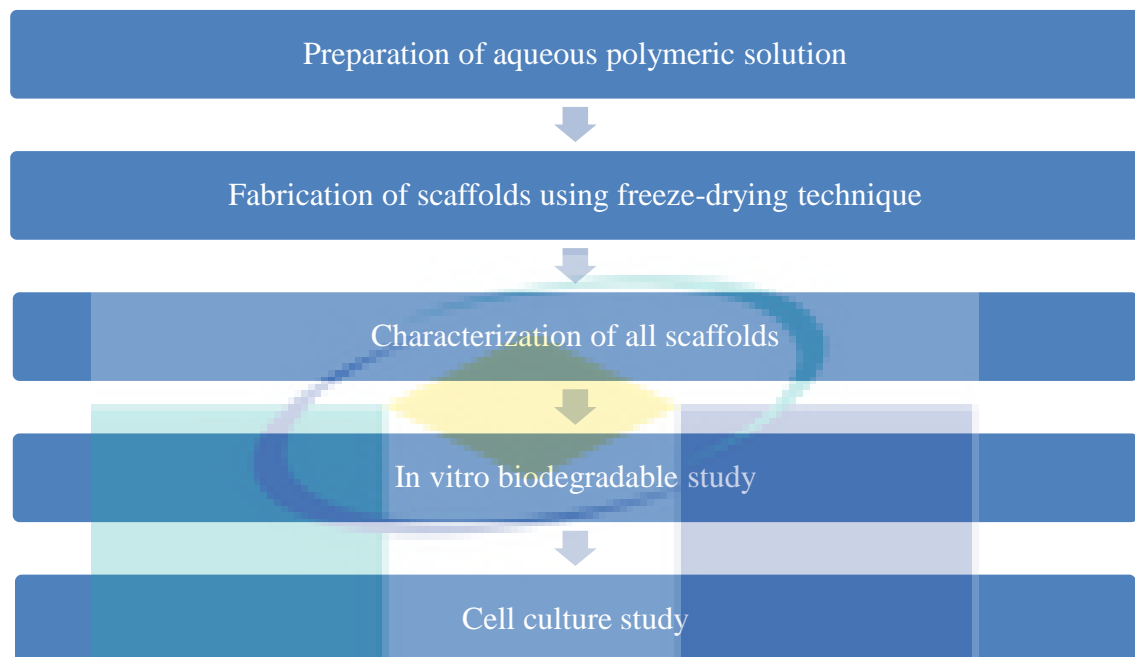


Figure 3.1 Summary of research methodology implemented in this research

UMP

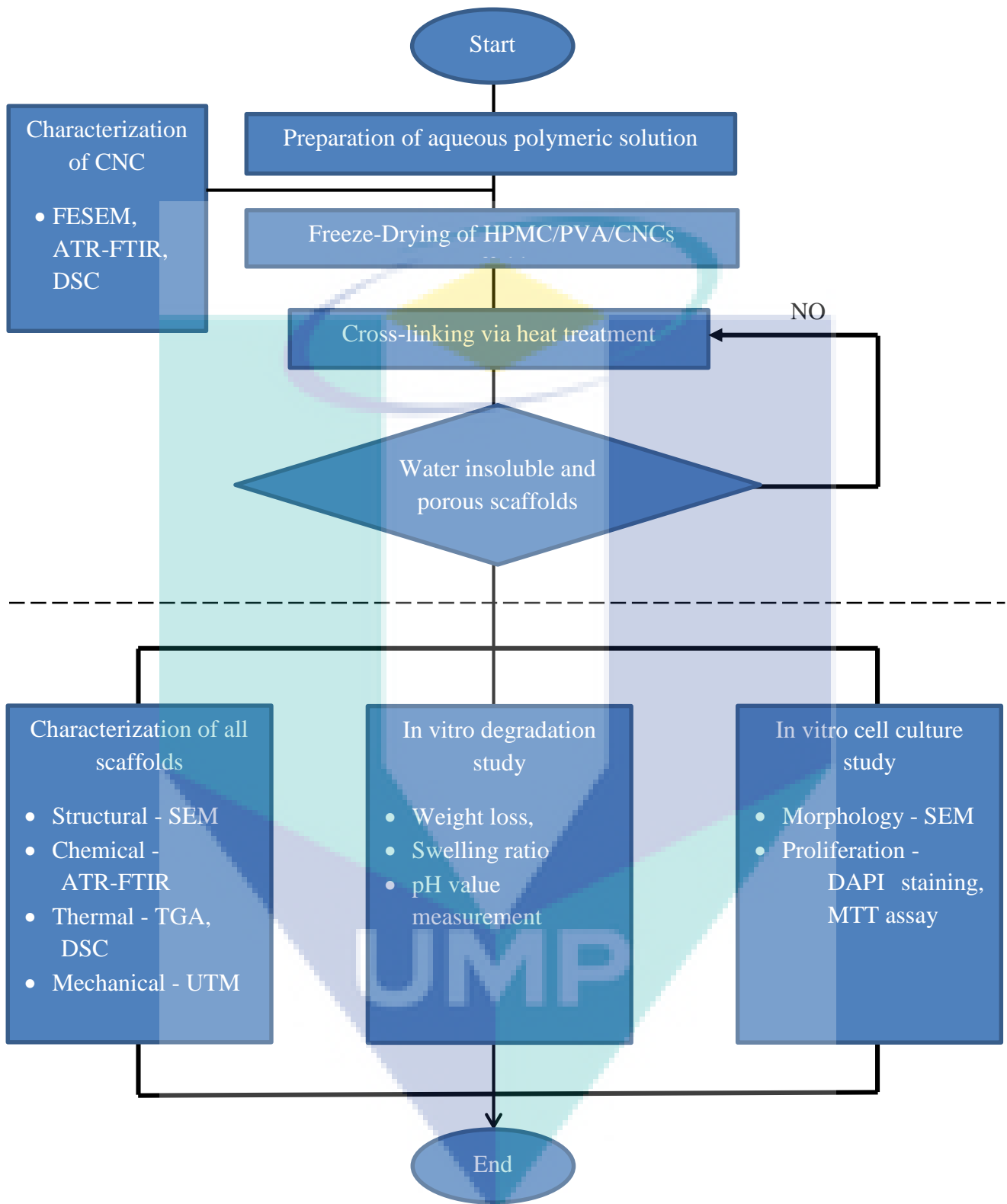


Figure 3.2 Flowchart of research methodology implemented in this research

### 3.2 Raw materials

PVA ( $M_w = 95,000$ ) was purchased from ACROS, New Jersey, USA. HPMC ( $M_w = 250,000$ ) and glutaraldehyde (GA) solution (25%) were purchased from Merck-Schuchardt, Germany. Cellulose was obtained Faculty of Sciences & Technology Industry, UMP. Phosphate buffer saline (PBS) was purchased from Gibco Life Technologies, USA and Dulbecco's Modified Eagle Medium (DMEM) was purchased from Life Technologies, USA. Human fetal osteoblast (hFOB) 1.19 (ATCC® CRL-11372™), SV4D large T antigen transfected was supplied from American Type Culture Collection (ATCC), USA for cell culture studies part. All chemicals were characterized by analytical purity and applied without further treatment. All the solutions were prepared using Millipore water.

### 3.3 Preparation of polymeric solution

Firstly, HPMC (5 wt%) solution was prepared by dissolving 5 g of HPMC powder in 100 ml of Millipore water and stirred for 14 h at room temperature until the solution became clear and thickened as the viscosity were slightly increased. In the meantime, 15 g of PVA granules were dissolved in 100 ml of Millipore water and stirred for about 2 h at 80 °C for fasten the time taken to dissolve the granules completely. PVA (15 wt%) solution were kept cool at room temperature and stirred continuously for another 12 h to ensure complete mixing. Then, HPMC and PVA solution were mixed together with ratios 50:50 and then stirred overnight to get a homogeneous mixture. Finally, cellulose suspension as shown in Figure 3.3 was added into HPMC/PVA blended polymer with different concentration for ternary blend system and stirred continuously for 24 h to get homogenous blend solution. The compositions of HPMC/PVA modified with CNCs are presented in Table 3.1.



Figure 3.3 Cellulose



Table 3.1 Composition of CNCs in HPMC/PVA blended polymer

HPMC (ml)	PVA (ml)	CNC (ml)	CNC (wt%)
75	75	0	0
		1.5	1
		4.5	3
		7.5	5
		10.5	7

### 3.4 Fabrication of HPMC/PVA/CNC porous material using freeze-drying method

Freeze-drying or lyophilization is the process of drying materials in the frozen state. This fabrication method is widely used especially in the laboratory and in industrial processes for the concentration, storage, and distribution of biological materials. Samples to be lyophilized should be aqueous solutions and there is a variety of containers are suitable for lyophilization. A proper container should withstand the outside pressure during lyophilization under high vacuum, and should be made of a material that allows a reasonable transfer of heat from outside to inside. The most commonly used containers in the laboratory are glass ampules and round-bottom flasks.

During freeze-drying, there were basically involved in three main steps which are freezing, primary drying and secondary drying. At freezing step, the polymeric solutions were frozen at a low temperature in the freezer. Then, at the primary drying step, the temperature was raised under vacuum where the water is removed by direct sublimation from the frozen samples in freeze-drying machine. In order to have a good freeze-drying practice and to avoid samples from collapse, it is better to keep the product temperature below the glass transition temperature ( $T_g$ ) or slightly higher collapse temperature ( $T_c$ ) of the product during primary drying (Kasper, Winter, & Friess, 2013). At the final step, which is secondary drying step, the elimination of the adsorbed water from the sample were occurred, which did not sublime upon primary drying because was not previously separated as ice during freezing (Fonte et al., 2016).

In this recent research, the scaffolds were fabricated by pouring the aqueous polymeric solutions into the falcon tube and kept in a deep freezer at  $-80\text{ }^{\circ}\text{C}$  for 24 h. Then, the samples were lyophilized at  $-50\text{ }^{\circ}\text{C}$  for 72 h in a freeze-dryer (FreeZone 6 Liter Benchtop Freeze Dry System, Labconco) as shown in Figure 3.4.

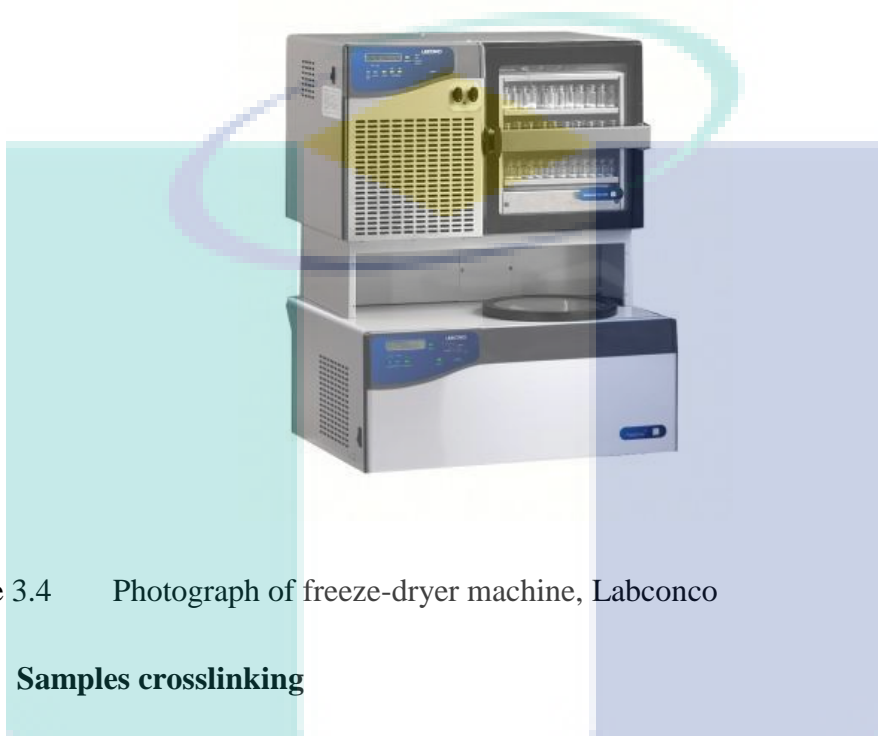


Figure 3.4 Photograph of freeze-dryer machine, Labconco

### 3.5 Samples crosslinking

Thereafter, the samples underwent heat treatment at  $80\text{ }^{\circ}\text{C}$  for 30 minutes in a vacuum oven. Water resistance of the scaffolds was evaluated in which the scaffolds were taken off from the falcon tube and then immersed them in distilled water. After proving that the scaffolds were not soluble or degrade in a short period of time, all the samples were dried in a vacuum oven and then kept in the dry box for further use.

### 3.6 Characterization of CNC nanoparticle and HPMC/PVA/CNCs scaffolds

FESEM is carried out to observe the morphology of CNCs. Meanwhile, SEM is used to observe the morphology HPMC/PVA/CNCs blended scaffolds. ATR-FTIR is performed to chemically confirm the presence of CNCs inside the matrices of HPMC/PVA. The thermal and mechanical properties were measured by DSC, TGA and UTM to evaluate the effect of CNC in HPMC/PVA.

### 3.6.1 Field emission scanning electron microscope (FESEM)

FESEM is a powerful instrument for analyzing topographic at nano-scale levels. It uses windows XP-based computerized operating system with high-resolution digital processing capacity. In this present study, the dimensions of CNCs nanoparticles were observed using FESEM. Figure 3.5 shows the JSM-7800F Extreme-resolution Analytical FESEM that has been used in this research. This equipment provides images at very high magnification and resolution (1.3 nm @ 30 kV). For this study, the range of magnification used is between 10 000x to 150 000x.



Figure 3.5 Photograph of FESEM, JSM-7800F Extreme-resolution Analytical

### 3.6.2 Scanning electron microscope (SEM)

The observation on the morphology and porosity of the lyophilized scaffolds can be easily carried out by SEM. In bone tissue engineering, study on the surface of scaffolds is important to observe the actual morphology, pore structure and adherence of cells, as initial indications of potential tissue scaffolds.

The FEI ESEM Quanta 450 FEG is a versatile scanning electron microscope with three imaging modes which are high vacuum (HV), low vacuum (LV) and ESEM (ESEM) mode. HV mode is a conventional SEM mode with the need of conventional

specimen preparation, while in the LV mode electrically non-conductive samples can be imaged without the need of a conductive layer such as carbon and gold. Whereas, in the ESEM mode, wet samples can be investigated in their natural state. The thermally assisted field emission gun (FEG) delivers high brightness of the electron beam and high imaging resolution.

In this present study, the surface morphology of all scaffolds were observed using FEI QUANTA 450 as shown in Figure 3.6 at an accelerating voltage of 15 kV. To have a better SEM images without giving bad effect to the images produced especially on scaffold's pore size, the scaffolds need to be cut right after applying liquid nitrogen all over the materials. Then, the samples were sputter coated with a thin layer of platinum in double 30 s consecutive cycles at 45 mA to reduce charging and produce conductive surfaces. Based on the SEM images produced, the pore sizes were analyzed using image visualization software, ImageJ.

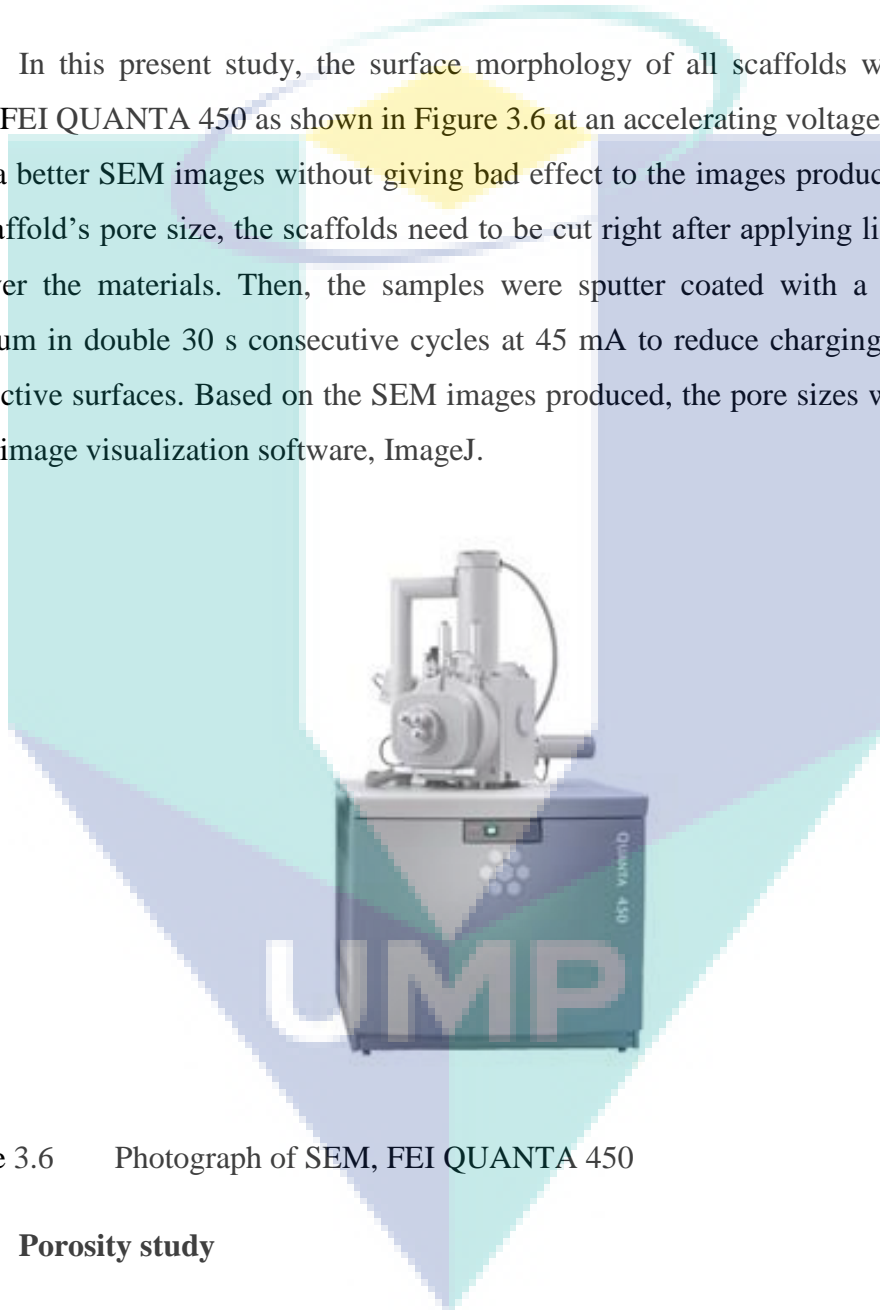


Figure 3.6 Photograph of SEM, FEI QUANTA 450

### 3.6.3 Porosity study

The porosity of scaffolds was measured by using liquid displacement method. All samples were cut  $1\text{ cm} \times 1\text{ cm} \times 1\text{ cm}$ , weighed and then immersed in deionized water as the displacement liquid for 30 min in a falcon tube. This method is based on the known volume before immersed of sample ( $V_1$ ) in a falcon tube, the unknown volume after 30 min immersed sample ( $V_2$ ) and the volume after removing of

impregnated sample ( $V_3$ ). The porosity of the sample can be calculated by the equation 3.1.

$$\text{Porosity (100\%)} = \frac{V_1 - V_3}{V_2 - V_3} \times 100\% \quad (3.1)$$

#### 3.6.4 Attenuated total reflectance-Fourier Transform Infrared Spectroscopy (ATR-FTIR)

Fourier Transform Infrared Spectroscopy (FTIR) is based on electromagnetic-wave absorption due to molecule vibrations. Characteristic IR-spectra of solid and liquid samples provide qualitative and semi-quantitative analyses. Two techniques are used for solid analyses which are Attenuated Total Reflection (ATR) and Potassium Bromide Disk method. In this study, ATR-FTIR spectroscopic analysis of scaffolds was performed on Spectrum One (Perkin-Elmer, USA) spectrophotometer, as shown in Figure 3.7, over a range of 700 to 4000  $\text{cm}^{-1}$  at a resolution of 2  $\text{cm}^{-1}$  with 100 scans per sample. This characterization was important to ensure the functional group of individual and the effect of blended HPMC, PVA, and CNCs on their intensities and peaks in the ATR-FTIR spectrum.



Figure 3.7 Photograph of ATR-FTIR, Perkin-Elmer.

#### 3.6.5 Thermogravimetric (TGA) analysis

TGA is used basically to investigate the thermal stability or better known as the strength of the material at a given temperature, oxidative stabilities where the oxygen absorption rate on the material, and the compositional properties such as fillers,

polymer resin, solvents of the samples. In modern TGA, it performs to determine the quantity and the frequency of the weight variation of the samples against temperature and time in a controlled atmosphere.

Typically, a TGA instrument offers a temperature range from 1000 to 1600 °C and the heating rate can be set from a range of a few decimal places to hundreds of °C/min. However, typical heating rate is between 1 and 20 °C/min, with very fast (>20 °C/min) or very slow (<1 °C/min) rates used only for some special reactions. The resolution of the thermogram can be controlled by the programmed heat rate, and usually the slower the heating rate the higher the resolution of the curves (Ng et al., 2018).

Differential thermal analysis (DTA) is usually incorporated with TGA to measure the temperature difference between a sample and a reference material as a function of temperature as they are heated or cooled or kept at a constant temperature. This differential temperature is then plotted against time or temperature. Changes in the sample, either exothermic or endothermic, can be detected relative to the inert reference. Consequently, the DTA curve may provide data on the transformations that have occurred such as glass transitions, crystallization, melting and sublimation.

In this present research, thermal analysis of scaffolds was performed using Q500 (TA instruments, New Castle, USA). Each sample was heat treated from 30 to 750 °C at a heating rate of 10 °C/min with nitrogen as purge gas.



Figure 3.8 Photograph of TGA, Q500.

### 3.6.6 Differential scanning calorimetry (DSC)

Due to its versatility and the high significance of its analytical output, differential scanning calorimetry (DSC) is the most often employed method for thermal analysis. DSC can be used to obtain thermal critical points like the temperatures of melting point ( $T_m$ ), crystallization ( $T_c$ ), or glass transition ( $T_g$ ), of the sample. The DSC 214 Polyma instrument from NETZSCH as shown in Figure 3.9 can be used to test on different types of samples such as powdered or compact solid, films and fibers at a broad temperature range from  $-180^{\circ}\text{C}$  to  $1750^{\circ}\text{C}$ .



Figure 3.9 Photographs of DSC, NETZSCH

Glass transitions may occur as the temperature of an amorphous solid is increased. These transitions appear as a step in the baseline of the recorded DSC signal. This is due to the sample undergoing a change in heat capacity; no formal phase change occurs. As the temperature increases, an amorphous solid will become less viscous. At some point the molecules may obtain enough freedom of motion to spontaneously arrange themselves into a crystalline form. This is known as the cold crystallization temperature. This transition from amorphous solid to crystalline solid is an exothermic process and results in a peak in the DSC signal. As the temperature increases the sample eventually reaches its melting temperature. The melting process results in an endothermic peak in the DSC curve. The ability to determine transition temperatures and enthalpies makes DSC a valuable tool in producing phase diagrams for various chemical systems. The output data displays a thermogram of heat flow ( $dQ/dt$ ) against temperature as shown in Figure 3.10;  $\Delta H$  is the estimated area of the DSC peak.

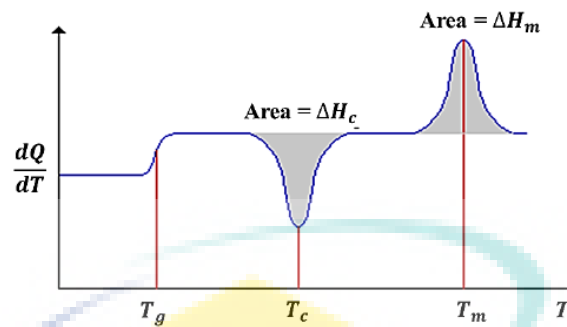


Figure 3.10 DSC thermograms

In this work, about 5 mg of sample was heat-treated from 50 to 250 °C at a heating rate of 10 °C/min, under atmospheric conditions. The degree of relative crystallinity,  $\chi_c$  can be expected from the endothermic area by the following equation:

$$\chi_c = \Delta H_f / \Delta H_f^\circ \quad (3.2)$$

where,  $\Delta H_f$  = measured enthalpy of fusion from DSC thermograms and  $\Delta H_f^\circ$  = enthalpy of fusion for 100 % crystalline polymer, which in this case is PVA=138.6 J/g (Merrill, 1976)

### 3.6.7 Mechanical properties

Mechanical testing such as hardness, tensile strength and compressive strength is important in bone tissue engineering application. Basically, this testing involved by applying a certain tensile force to a sample with known dimension, clamping at the end of the sample and the sample will be stretching after the system is running. The system stops automatically when the materials achieve break point. In this recent research, the mechanical properties of the scaffolds were measured using a universal testing machine (UTM) (Autograph AGS-X series, Shimadzu) as shown in Figure 3.11. The samples were cut in rectangular shape with same dimensions for all scaffolds. The room conditions were controlled at 25 °C and 34% humidity. The speed rate used is 10 mm/min. The AGS-X comes standard with industry-leading TRAPEZIUM X data



processing software. The tensile stress and strain at break were calculated based on the obtained tensile stress-strain curve.

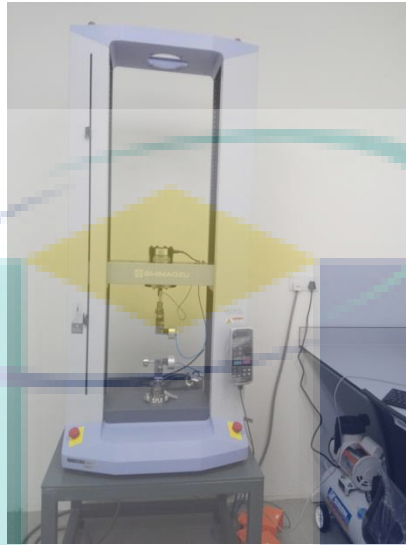


Figure 3.11 Photograph of universal testing machine, Shimadzu

### 3.7 In vitro degradation study

This study was focused on the degradation behavior of HPMC/PVA/CNCs porous scaffolds, as potential substrates for bone tissue engineering in a biologically related media which is phosphate buffered solution (PBS). The scaffolds were characterized at different degradation times by a series of analysis including swelling ratio, weight loss and pH changes.

#### 3.7.1 Swelling ratio study

All scaffolds were cut into 1 cm x 1cm x 1cm and placed in falcon tube. The scaffolds were weighed ( $W_d$ ) before submerged in PBS. The solution needs to be maintained at 37°C throughout the analysis. The wet weight of the samples ( $W_t$ ) was determined after 1, 3 and 7 days by gently blotting them on filter paper. The water uptake or swelling analysis was conducted in triplicates for all types of scaffolds. Swelling ratio was calculated according to Equation 3.3.

$$\text{Swelling ratio (\%)} = \frac{W_t - W_d}{W_d} \times 100 \% \quad (3.3)$$

### 3.7.2 pH value measurements

The pH value measurement was done for all scaffolds after the degradations at each time point were obtained by using a pH meter (Horiba LAQUA Handheld Water Quality Analysis Meters) as shown in Figure 3.12. Note that, pH value for PBS is 7.4.



Figure 3.12 Photograph of Horiba LAQUA Handheld Water Quality Analysis Meters

### 3.7.3 Weight loss study

Weight loss percentages were determined after drying the samples in vacuum by comparing the dry weight,  $W_d$  at a certain time point with the initial weight,  $W_0$  according to Equation 3.4.

$$\text{Weight loss (\%)} = \frac{W_0 - W_d}{W_0} \times 100 \% \quad (3.4)$$

The lyophilized scaffolds were cut into 1 cm x 1cm x 1cm, placed in Falcon tube containing 3 ml of PBS and incubated at 37°C. The samples were then taken out at different periods of time which is at 1, 3 and 7 days. After testing, the scaffolds were washed with distilled water and kept dry in a desiccator for further use.

### 3.8 Cell culture study

The cell culture studies were carried out to examine the interaction of cell with the prepared scaffolds. Figure 3.13 shows the basic step for cell culture where the primary cells were expanded in tissue culture flask at first, then underwent subculture and finally, seeded on the scaffolds.

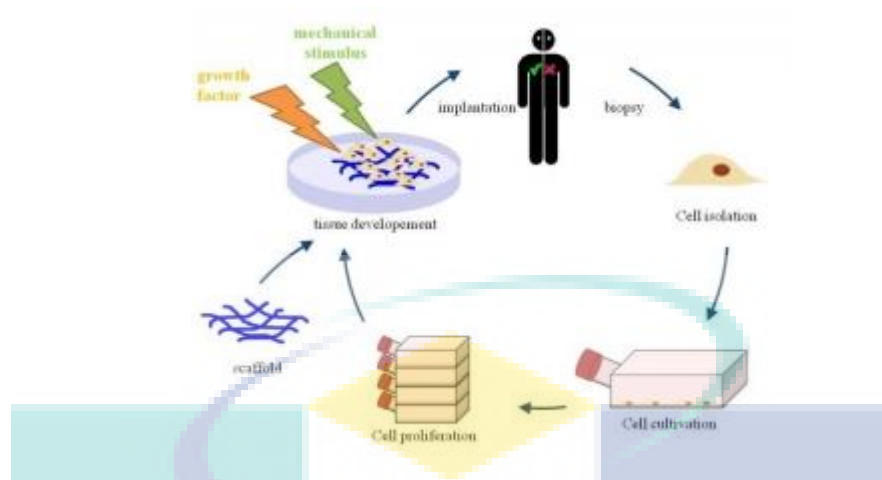


Figure 3.13 Summarize of cell culture study

### 3.8.1 In vitro cell culture study of HPMC/PVA/CNC scaffolds

Human fetal osteoblast (hFOB) cells is cultured, expanded and seeded on HPMC/PVA/CNC scaffolds. The cells-scaffolds were incubated to facilitate cells growth and observe after 1, 3, 5 and 7 days. The cell proliferation is measured by DAPI staining and MTT assay while the morphology of hFOB cells on scaffolds were observed under SEM.

### 3.8.2 hFOb cells expansion and seeding

Firstly, the scaffolds; HPMC/PVA, HPMC/PVA/CNC (1,3,5,7 wt%) were cut into small disks with 10 mm diameter, soaked in 100 % ethanol for 24 h, and then sterilized under UV light for 3 h and subsequently immersed in cell culture medium, Dulbecco's modified Eagle's medium (DMEM) solution. Then, the scaffolds were kept in incubator at 37 °C in 5% carbon dioxide (CO<sub>2</sub>) humidified atmosphere for five days. All changes were observed including the pH of media before and after five days in the incubator. Finally, the scaffolds were washed thrice with sterile PBS and transferred into a 24-well tissue culture plate.

hFOB cell lines were propagated in Dulbecco's modified Eagle's medium (DMEM) in a cell culture flask, all supplemented with 10% fetal bovine serum and 5% penicillin/ streptomycin and maintained at 37 °C in 5% carbon dioxide (CO<sub>2</sub>) humidified atmosphere.

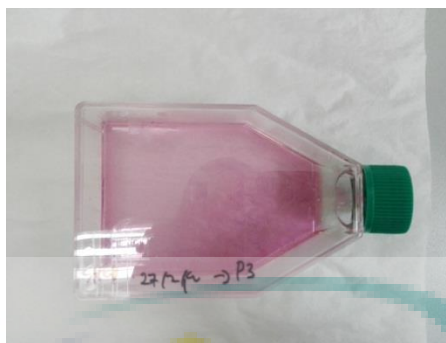


Figure 3.14 hFOB cell in cell culture flask

It is crucial to maintain and feeding the hFOB cell regularly and routinely. The cell morphology, color, and turbidity were checked by microscope to ensure there is no presence of contaminants. DMEM solution was changed once for each two days to avoid the cells from depleting, depriving of specific nutrients, or becoming acidic. For media changing, the spent media was removed and equal volume of fresh media (5 ml) was added to the cell culture flasks. The flasks were stored and maintained in 5% carbon dioxide (CO<sub>2</sub>) humidified atmosphere at 37 °C in the incubator.

In order to perform subculture of cell, hFOB cells were passaged when they have reached 80-90% confluence of the surface area of a flask to maintain healthy growth. DMEM solution were removed and discarded. Then, TrypLE solution was added to cell culture flask to detach the cells and swirled across the adhered cells to ensure it reaches all cells. The detachments of the cells were checked by using microscope after the flasks being incubated for about 5 minutes. Once the cells were detached from the flask, the cell suspensions were transferred into 15mL tube and centrifuged at 800rpm for 5 minutes. Finally, TrypLE solution was removed and fresh DMEM solution containing serum was then added to inactivate the TrypLE solution in the cell suspension.

The aliquot of cell suspensions were placed into a new flask containing 5 mL of DMEM solution, then stored in the incubator. After 24 hours, the cultures were checked to ensure that cells were reattached. The medium was changed as necessary until the next subculture. The cell-scaffolds were incubated in 24-well plate at different time points as shown in Figure 3.15.

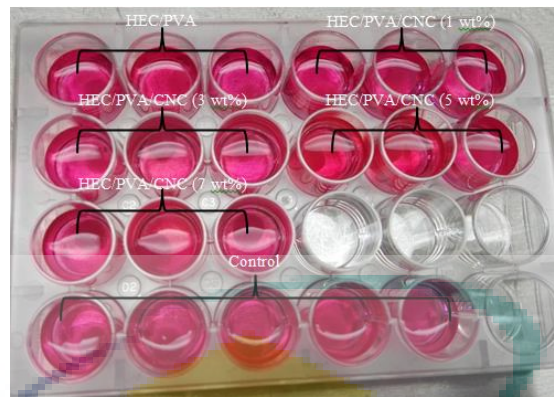


Figure 3.15 Cell culture studies of scaffolds at different weight ratios

### 3.8.3 hFOb cells morphology studies

After the cell is cultured, hFOB cells grown on scaffolds were rinsed twice with PBS and fixed in 3% GA for 30 min. Thereafter, the scaffolds were dehydrated with increasing concentrations of alcohol (20, 40, 60, 80 and 100%). The samples were air dried by keeping the samples in a fume hood. Lastly, the scaffolds were observed using SEM at an accelerating voltage of 10 kV.

### 3.8.4 hFOb cells proliferation study

In order to perform the proliferation assay for hFOB cell, at least 5,000 or  $5 \times 10^3$  cells per well are recommended. In this study, the cells were distributed in 24-well cell culture plates at a concentration of approximately  $10 \times 10^3$  cells prior adding the scaffolds in each different well with DMEM solution. The proliferation test was observed by images taken from EVOS inverted microscope for 1, 3, 5 and 7 days at 10x magnification by using Trypan blue staining.



### 3.16 Photograph of EVOS inverted microscope

DAPI (4,6-diamidino-2-phenylindole) staining also had been done to detect nucleus cells using fluorescent microscope. The cell-scaffolds were washed three times in PBS solution. About 300 nM DAPI stain solution were added to cover the cells and incubated for 5 minutes, protected from light. The stain solutions were removed and the cell-scaffolds were washed again in PBS solution. By using fluorescent microscope, the images of the cell were observed.

On the other hand, MTT assay test was carried out by measuring the reduction of the yellow tetrazolium salt to purple formazan crystals by dehydrogenase enzymes secreted from the mitochondria of metabolically active cells. The amount of the purple formazan crystals formed is proportional to the number of viable cells. For this study, 150  $\mu$ L of Dimethyl sulfoxide (DMSO) solvent was added into each of the cell-scaffolds to dissolve the MTT formazon crystal. The well plate was placed in a NanoQuant micro plate reader (infinite M200PRO) to detect biological, chemical or physical events of samples by using emitting light. The absorbance was recorded at 570 nm with background 630nm representing the number of viable cells was measured. For data analysis, the cell proliferation is calculated using the following formula:

$$\text{Cell viability (\%)} = \frac{(A_{\text{sample}} - A_{\text{blank}}) - (A_{\text{control}} - A_{\text{blank}})}{(A_{\text{control}} - A_{\text{blank}})} \quad (3.5)$$

where  $A_{\text{sample}}$  = absorbance at 570 nm of the sample,  $A_{\text{control}}$  = absorbance at 570 nm of the positive control which is cells in complete medium incubated in the absence of the scaffolds and  $A_{\text{blank}}$  = background absorbance of the blank wells. An average of triplicate reading was calculated for each sample.



Figure 3.17 Photograph of NanoQuant micro plate reader (infinite M200PRO)

UMP

## CHAPTER 4

### RESULTS AND DISCUSSION

#### 4.1 Characterization of CNC

In this section, we discuss the characterization of nanomaterials to be used in bone tissue engineering based on its morphology, chemical and thermal properties. CNCs, currently used or with potential applications in tissue engineering acts as a nanofiller in producing porous scaffolds.

##### 4.1.1 Morphology of CNC

Morphology of nanocellulose is one of the most important parameters to control during production and it depends on the cellulose source and the production method. In the case of CNC, different microscopic techniques suggested that they are rod-shaped with remarkable uniform width but a wide distribution of lengths. From Figure 4.1, the spherical CNC were loosely packed while the isolated spherical cellulose nanocrystals in ~30nm diameters were observed by FESEM.

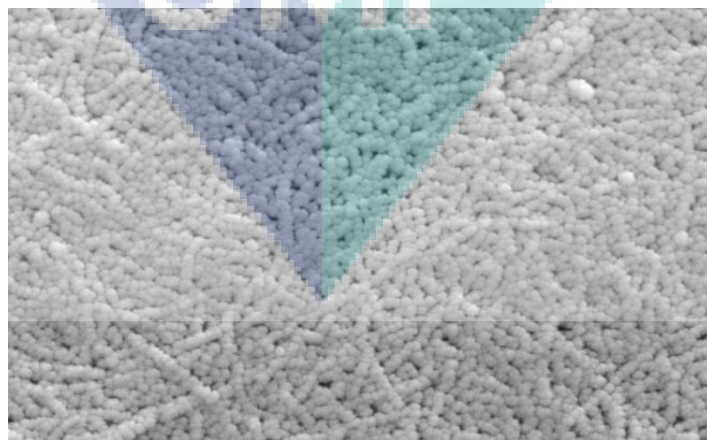


Figure 4.1 FESEM micrographs of CNC nanocrystals at 50,000x



### 4.1.2 Chemical properties of CNC

The chemical properties of CNC were carried out using ATR-FTIR. From the figure the analysis, the absorption at  $2895\text{ cm}^{-1}$  refers to the aliphatic saturated C-H stretching, associated with methylene groups in cellulose. Ring stretching vibrations (C=C stretching) occurs at  $1576\text{ cm}^{-1}$ . At FTIR spectra of  $1040\text{ cm}^{-1}$ , C-O stretching of alcohol. The strong bond was obtained at  $3340\text{ cm}^{-1}$  region due to the O-H stretching vibration.

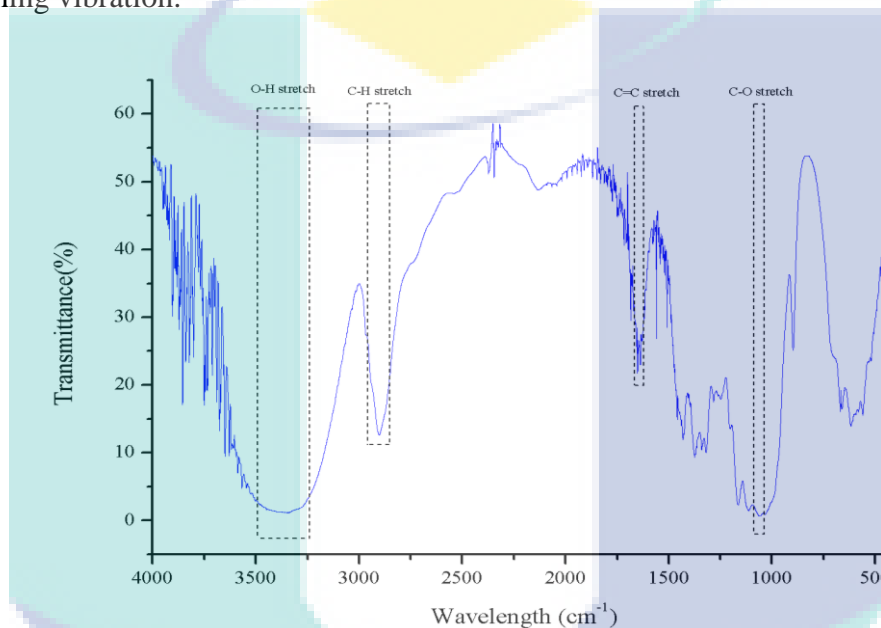


Figure 4.2 ATR-FTIR analysis of CNC nanocrystals

### 4.1.3 Thermal study of CNC

Thermal properties is one of the most important properties affecting the performance of nanocellulose particles in different applications, such as imaging and drug delivery. CNC can not only improve the thermal stability of produced scaffolds but also they can increase degradation stability in different fluids. Thermal stability of CNC was better due to the introduced of sulphate groups into CNC by hydrolysis with acid sulphuric. The sulphate groups at the outer layer of cellulose during acid hydrolysis caused dehydration of cellulose fiber to reduce the thermal stability. From the analysis, melting temperature ( $T_m$ ) is at  $197.1\text{ }^\circ\text{C}$ , while the glass transition temperature ( $T_g$ ) is  $65.2\text{ }^\circ\text{C}$ .

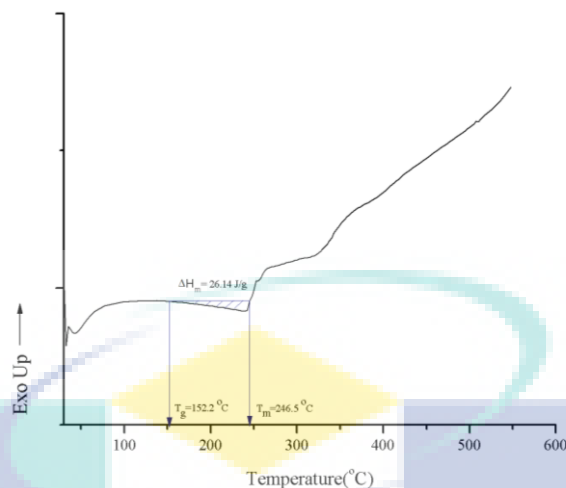


Figure 4.3 DSC thermograms of CNC nanocrystals

#### 4.2 Characterization of HPMC/PVA and HPMC/PVA/CNCs scaffolds

Figure 4.4 shows the polymeric solution of HPMC/PVA and HPMC/PVA/CNC (1, 3, 5, and 7 wt%). All solutions were milky in color and as the concentration of CNCs increased, the solution became more cloudy. These polymeric solutions were then freeze-dried on a freezer at  $-80\text{ }^\circ\text{C}$ . After that, the samples were cross-linked using heat treatment in a microwave oven to increase the degradation time of the produced scaffolds. From Figure 4.5, all scaffolds were brittle but in a hard spongy-like structure.



Figure 4.4 HPMC/PVA and HPMC/PVA/CNC (1, 3, 5, 7 wt%) polymeric solutions

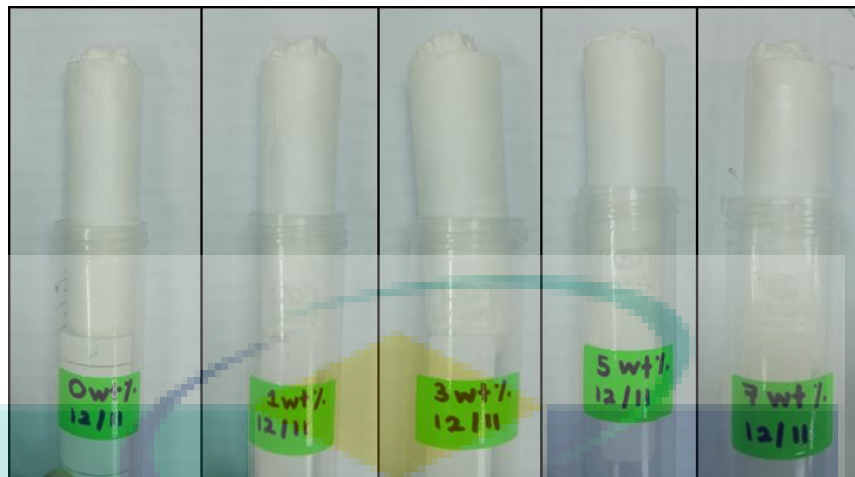


Figure 4.5 HPMC/PVA and HPMC/PVA/CNC (1,3,5,7 wt%) scaffolds

#### 4.2.1 Morphology of scaffolds

The microstructures of HPMC/PVA and HPMC/PVA/CNC (1, 3, 5, and 7 wt%) are illustrated as in Figure 4.6. From the SEM images, the produced scaffolds showed high interconnectivities between pores. By varying the concentration of CNC, a controllable pore size with particular wall structure could be obtained. The HPMC/PVA scaffold displayed large porous structure while HPMC/PVA/CNC scaffolds showed more open microstructure with interspacing pore. Morphology of HPMC/PVA/CNC scaffolds revealed a more porous structure with a three-dimensionally interconnection throughout the scaffolds in all compositions compared to HPMC/PVA scaffolds. The shrink-like structure appeared might be caused by the effect of heat treatment, which disturbed the round pores formation. Some micropores less than 10  $\mu\text{m}$  were also observed at higher magnification. These micropores could have been the result from the rapid sublimation by reduced surrounding pressure during freeze-drying. The existence of micropores is favourable since it might increase the interconnectivity and interface area of the porous scaffolds.

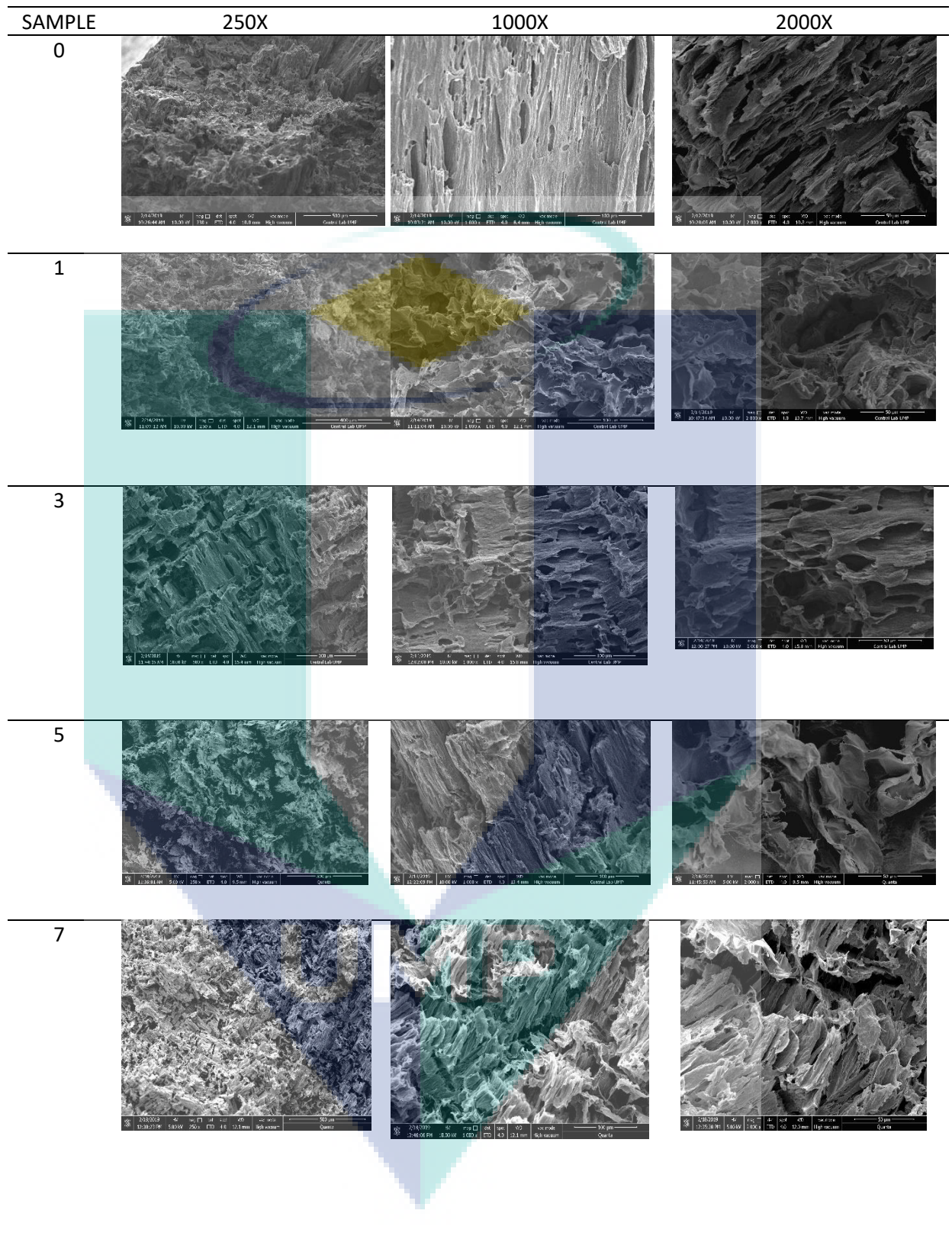


Figure 4.6 SEM micrographs of HPMC/PVA interconnected porous scaffolds with different CNC concentration at (1,3,5 and 7 wt%)

## 4.2.2 Porosity

Scaffold porosity is one of the important features to evaluate the biomaterial properties for tissue engineering. It is well-known that HPMC, PVA and CNC are water-soluble biopolymers, which are not favorable for cell culture studies. Therefore, cross-linking these materials is a must to decrease their solubility as well as to give mechanical strength for cell culture studies. In this report, porosity measurements of cross-linking scaffolds were completed by using liquid displacement method with deionized water as the displacement liquid.

As illustrated in Figure 4.7, all porous scaffolds show high porosity with percentage value above 77.49% at a maximum of 99.59 % for pure HPMC freeze-dried scaffolds. The results pointed that porosity of scaffold containing CNC decreases with the addition of CNC content due to the greater influence of the cross-linking mechanism among –OH groups of HPMC, PVA, and CNC. The morphology of three-dimensional scaffold structure should possess high porosity. Overall, these results suggested that high porosity of these scaffolds could be suitable for cell cultivation and transplantation in bone tissue bioengineering. In general, the scaffolds with higher porosity are likely to support greater cellular proliferation and infiltration in tissue engineering.

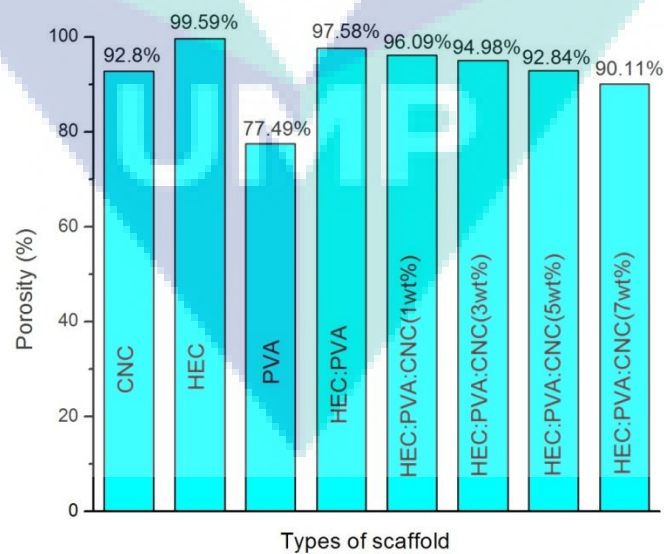


Figure 4.7 Porosity of CNC, HPMC and PVA alone and HPMC/PVA scaffolds with different CNC concentration at (1,3,5 and 7 wt%)

### 4.2.3 ATR-FTIR study

The attenuated total reflection-Fourier transform reflection (ATR-FTIR) spectra of pure HPMC, PVA, and CNC, blended HPMC/PVA and HPMC/PVA/CNC (1, 3, 5 and 7 wt%) cross-linked porous scaffolds is illustrated in Figure 4.8. FTIR spectra analysis was carried out to enlighten the presence of HPMC, PVA, and CNC inside the porous materials and to figure out the interaction occurs among them and to analyze the interaction (hydrogen bonding) between them.

Pure HPMC showed a broad peak at  $3376\text{ cm}^{-1}$  assigned to O-H stretching vibrations and  $2929\text{ cm}^{-1}$  assigned to C-H aliphatic stretching vibrations. The absorption spectra of HPMC presented specific bands in 1463, 1354, 1310 and  $932\text{ cm}^{-1}$  (Zhbakov, 1966), which corresponded to a characteristic of amorphous region and possible heterogeneity on the distribution of the replaced groups in the polymer chains (Kumar et al., 2012).

For pure PVA, a large band appeared at  $3303\text{ cm}^{-1}$ , representing the O-H stretching from the intermolecular and intramolecular hydrogen bonds while the vibrational bond at  $2944\text{ cm}^{-1}$  contributed to the stretching of C-H from alkyl groups of PVA. Strong peaks emerged at  $1709\text{ cm}^{-1}$  and  $1655\text{ cm}^{-1}$  referring to the stretching of C-O from acetate groups remaining in PVA, while peaks for  $1429\text{ cm}^{-1}$  were related to the bending vibrations of  $\text{CH}_2$ .

Meanwhile, the FTIR spectra for HPMC/PVA/CNC blended scaffolds showed the combination of major peaks of HPMC, PVA and CNC. It was found that the ratio of absorption intensities of C-H and O-H stretching increased with the addition of HPMC content. The broad pattern of blend scaffolds observed at O-H region ( $3313 - 3337\text{ cm}^{-1}$ ) and peak of C-H varied from  $2870$  to  $2939\text{ cm}^{-1}$ , which might be due to the rise in swelling ratio of the samples. The strong peaks observed from  $829$  to  $937\text{ cm}^{-1}$  exhibited the C-H and  $\text{CH}_2$  bending vibrations while peaks varied from  $1055$  to  $1059\text{ cm}^{-1}$  were assigned to C-O stretching, showing peaks with slight shift to the left with the increase of HPMC polymers. These results suggest that the  $\text{H}_2$  bonding becomes increased due to increased number of OH groups.

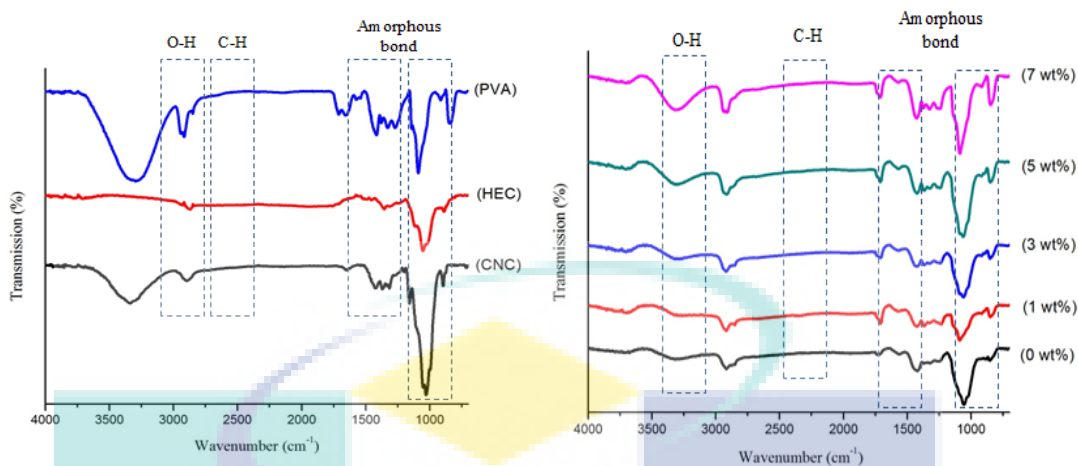


Figure 4.8 ATR-FTIR spectra of CNC, HPMC and PVA alone and HPMC/PVA scaffolds with different CNC concentration at (1,3,5 and 7 wt%)

#### 4.2.4 TGA measurements

Thermal stability of HPMC/PVA and HPMC/PVA/CNC scaffolds was studied using TGA. The thermograms and its derivatives (DTA) of all scaffolds are illustrated in Figure 4.9. All curves exhibited three major weight losses. These steps were distinguishable in the diagram of mass loss (TGA %) during heating as well as more clearly in the diagram of derivative mass loss (DTA %). The details of the decomposition step and percentage mass loss for HPMC/PVA and HPMC/PVA/CNC scaffolds are summarized in detail as shown in Table 4.1.

It is clear that all the scaffolds exhibited almost similar trends in their thermal properties. It is interesting to note that the shape of the TGA/DTA curves for the HPMC/PVA/CNC combines the main characteristics of HPMC, PVA and CNC with an initial steep decrease in slope (similar to CNC) followed by gradual degradation (similar to PVA). These TGA results provide further evidence to the successful fabrication of scaffolds via freeze-drying technique. The difference in thermal decomposition behavior of HPMC/PVA and HPMC/PVA/CNC blend samples can be seen more clearly from DTA curves. It can be concluded that the thermal stability of HPMC/PVA scaffold was increased by mixing it with CNC. The maximum mass loss rate of HPMC/PVA/CNC scaffolds shifted to a lower temperature compared with

HPMC/PVA scaffold, which indicate that CNC degraded at low temperature than HPMC/PVA scaffold.

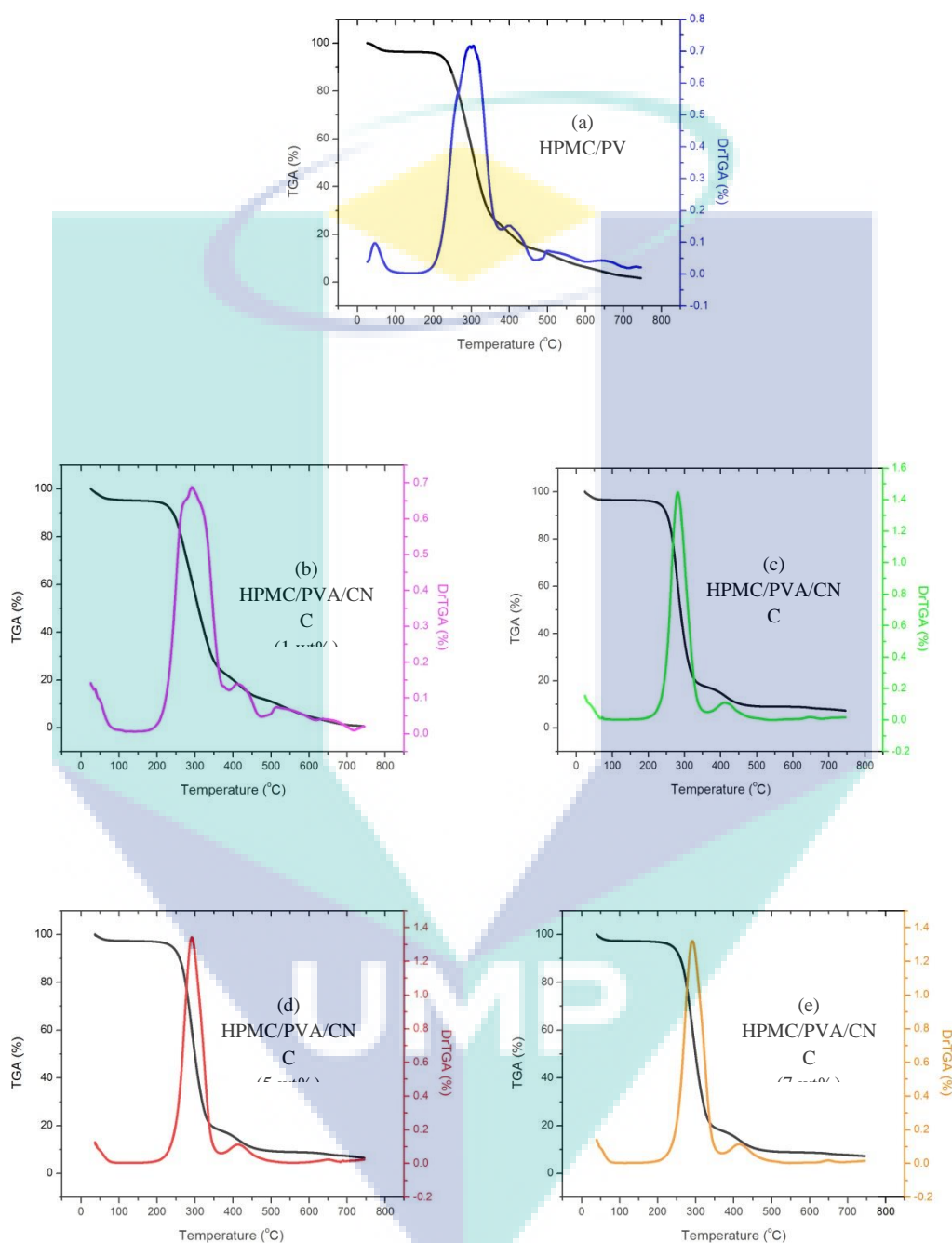


Figure 4.9 TGA and DTA curves for HPMC/PVA scaffolds with different CNC concentration at (1,3,5 and 7 wt%).



Table 4.1 TGA and DTA for all scaffolds

Sample	Region of decomposition	Temperature (°C)			Weight loss (%)	
		T <sub>start</sub>	T <sub>end</sub>	T <sub>peak</sub>	Partial	Total
HPMC/PVA	1 <sup>st</sup>	26	175	46	4.100	98.43
	2 <sup>nd</sup>	175	378	304	72.00	
	3 <sup>rd</sup>	378	465	400	22.33	
HPMC/PVA/CNC (1wt%)	1 <sup>st</sup>	25	190	140	5.438	97.548
	2 <sup>nd</sup>	190	387	290	71.26	
	3 <sup>rd</sup>	387	511	422	20.85	
HPMC/PVA/CNC (3wt%)	1 <sup>st</sup>	25	197	75	3.860	94.77
	2 <sup>nd</sup>	197	360	280	78.90	
	3 <sup>rd</sup>	360	494	412	12.01	
HPMC/PVA/CNC (5wt%)	1 <sup>st</sup>	36	196	149	3.044	93.574
	2 <sup>nd</sup>	196	358	291	79.05	
	3 <sup>rd</sup>	358	534	415	11.48	
HPMC/PVA/CNC (7wt%)	1 <sup>st</sup>	39	192	124	3.119	92.829
	2 <sup>nd</sup>	124	359	291	79.09	
	3 <sup>rd</sup>	359	509	418	10.62	

#### 4.2.5 DSC study

An important factor in the development of new materials based on polymeric blends is miscibility between the polymers in the mixture, because the degree of miscibility is directly related to final properties of polymeric blend. The glass transition temperature value of a polymer can be modified with a blending small amount of additive. This phenomenon is called plasticization. Thermograms for pure components and all porous scaffolds are shown in Figure 4.10.

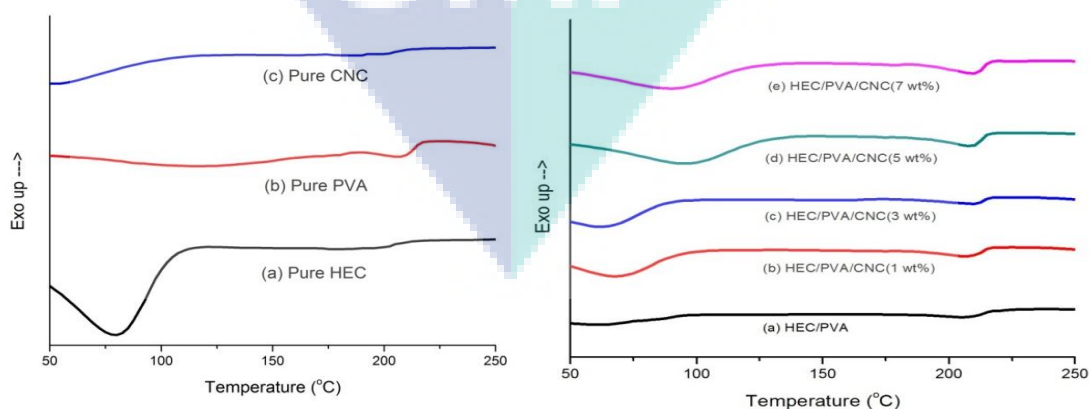
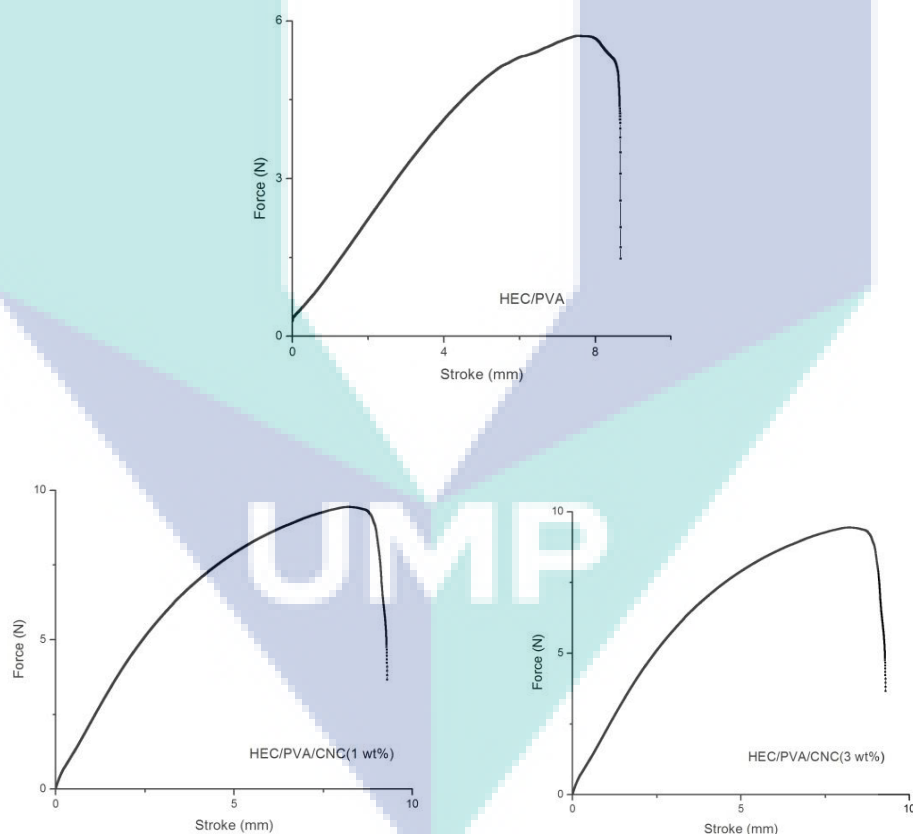


Figure 4.10 DSC thermograms of CNC, HPMC and PVA alone and HPMC/PVA scaffolds with different CNC concentration at (1,3,5 and 7 wt%)

#### 4.2.6 Mechanical properties

In the fabricated porous scaffolds, significant changes were observed in the linear elastic and plastic regimes with increasing CNC content, corresponding to improved cell wall strength with different mechanical behavior resulting in increased compressive strength (which is also associated with the porosity) of the fabricated porous scaffolds. The compressive strength and Young's modulus HPMC/PVA were 0.18 and 12.67 MPa, while incorporation with various concentration of CNC into the blended polymer increased the compressive strength and Young's modulus. These results suggest that CNC offers an improvement in the mechanical performance of the material. The combination of CNC in HPMC/PVA provides strength and stiffness to the final HPMC/PVA/CNCs scaffolds.



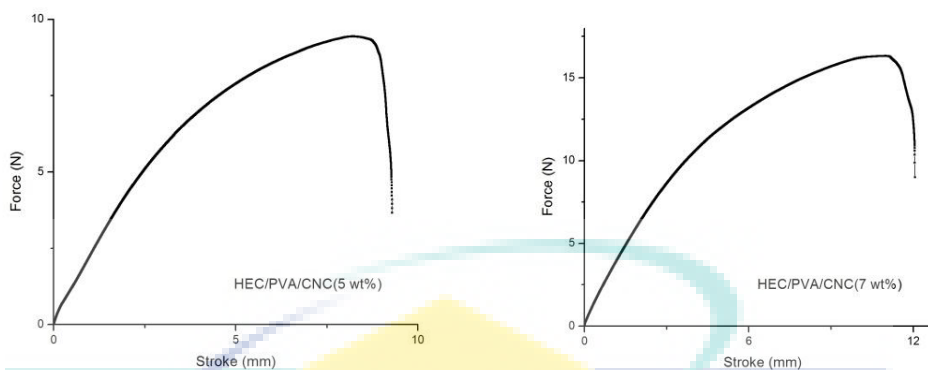


Figure 4.11 Compressive strength for HPMC/PVA scaffolds with different CNC concentration at (1,3,5 and 7 wt%)

Table 4.2 Compressive strength and Young's modulus for all scaffolds

Type of scaffolds	Compressive strength (MPa)	Young's modulus (MPa)
HPMC/PVA	0.18	12.67
HPMC/PVA/CNC (1 wt%)	0.25	18.04
HPMC/PVA/CNC (3 wt%)	0.43	30.25
HPMC/PVA/CNC (5 wt%)	0.45	31.63
HPMC/PVA/CNC (7 wt%)	0.92	52.85

### 4.3 In vitro degradation study of HPMC/PVA and HPMC/PVA/CNCs scaffolds

The degradation behavior of porous scaffold is important criteria that need to be stressed. Scaffolds should be biodegradable in order to work well in human body system. Hence, weight loss, swelling ratio and pH value analysis were carried out in this research.

### 4.3.1 Weight loss, swelling ratio and pH value analysis

The amount of water in hydrogel enables the determination of absorption or/and diffusion of solutes through the hydrogel. The equilibrium swelling ratios of the prepared pure HPMC, blended HPMC/PVA and pure PVA scaffolds are illustrated in Figure 4.12, as a function of polymer composition. After the day 1 experiment, all scaffolds showed high degree of swelling ratio, reflecting the hydrophilic properties of the scaffolds; i.e., highly porous network enables the absorption of an amount of bulky water. The values of swelling ratio of all scaffolds increased parallel throughout the 7 days of experiment. It is worth to note that after 7 days, at some time point, the swelling capability of the scaffolds will achieve maximum swelling capacity and will ultimately start to degrade due to the breaking of polymer chains (Erol et al., 2012).

In tissue engineering, porous biodegradable scaffolds are said to facilitate and provide sufficient spaces for cell growths and tissue formation. The degradation of scaffolds in PBS at 37 °C over 7-day incubation was evaluated. All scaffolds exhibited increment in percentage of degradation with time.

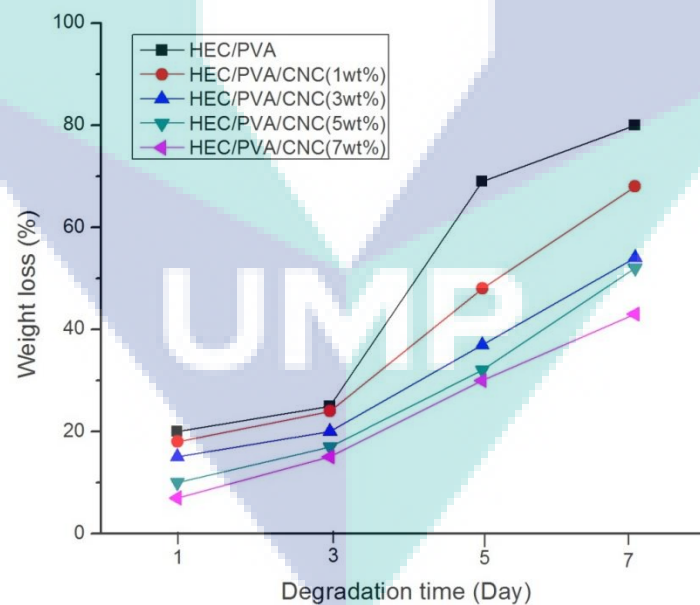


Figure 4.12 Weight loss for HPMC/PVA scaffolds with different CNC concentration at (1,3,5 and 7 wt%)

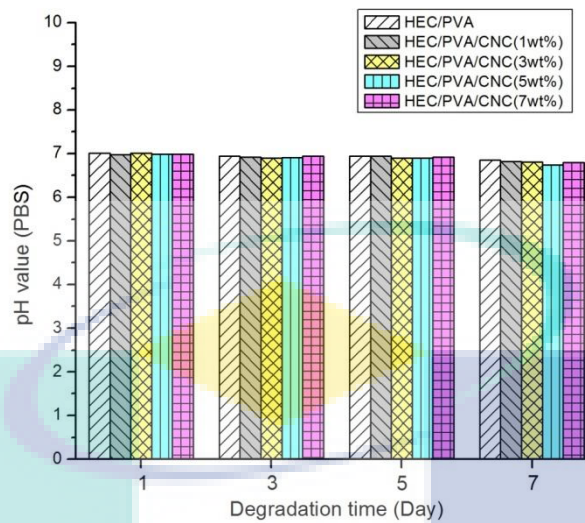


Figure 4.13 pH value analysis of HPMC/PVA and HPMC/PVA/CNC (1, 3, 5, 7 wt%) porous scaffolds.

#### 4.4 Cell culture studies on HPMC/PVA and HPMC/PVA/CNCs for bone tissue engineering applications

Cell culture experiment is conducted to test the toxicity and biocompatibility of the materials towards the living cells. Generally, good biocompatibility requires the cells to attach and grow well internally and externally of the scaffolds. Hydroxyapatite is the major inorganic component present in human bone that is often integrated in a scaffold for bone regeneration because of its biocompatibility and osteoconductive properties and as a neutralizing additive due to its alkaline property. Attentions were focused on the morphology, viability and proliferation of human fetal osteoblast cells (hFOB) on scaffold.

##### 4.4.1 hFOB cells proliferation on scaffolds

The viability of hFOB cells cultured on scaffolds was measured by an MTT cell proliferation assay, and the number of viable cells was assayed by cell counting under an inverted fluorescence microscope. The intrinsic mechanism of the MTT assay is that active cells react with a tetrazolium salt in the MTT reagent to produce a soluble formazan dye, which can be absorbed at a wavelength of 490 nm. The results obtained

by MTT assay were compared with hFOB cells in a complete media without the presence of scaffolds as a positive control.

According to the results, there were no significant difference in biocompatibility between control and all scaffolds after 7 days. Though there was no significant difference in the proliferation of osteoblast cells in all porous scaffolds, HPMC/PVA/CNC scaffolds shows more osteoblast cell proliferation compare to HPMC/PVA scaffold.

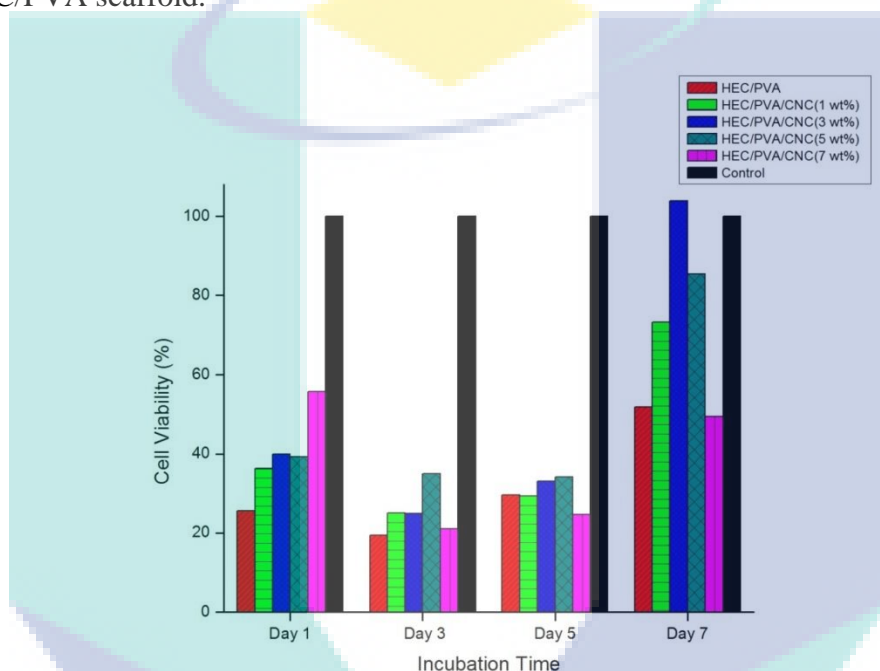
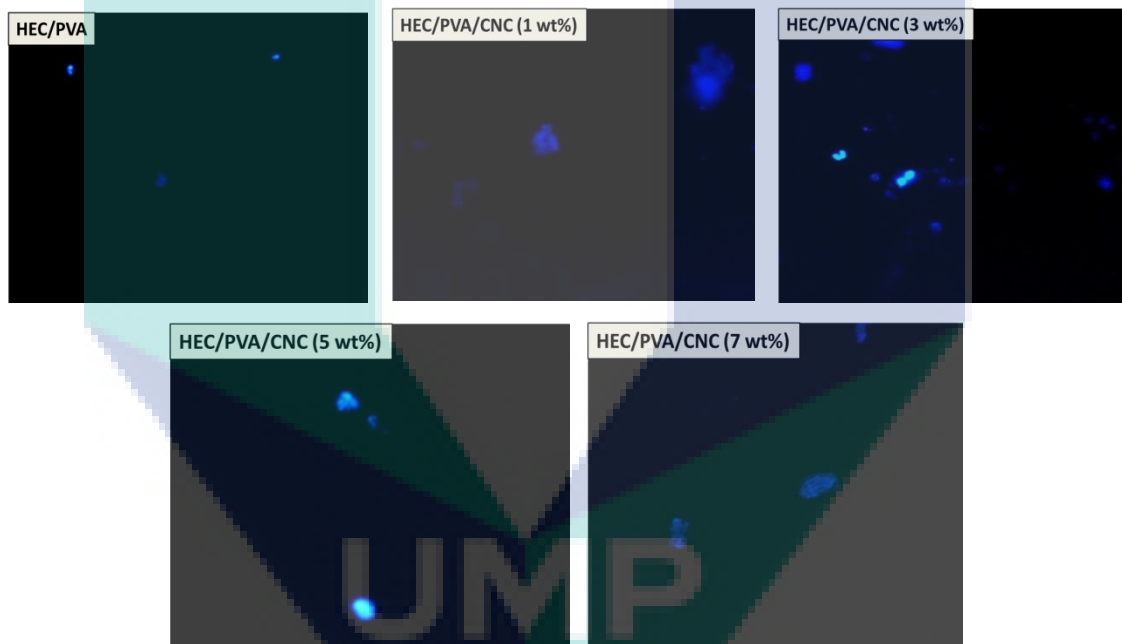


Figure 4.14 Graph showing human osteoblast viability after 1, 3, 5 and 7 days of incubation ( $1 \times 10^5$  cells/well in complete DMEM) at different weight ratios of scaffolds.

Figure 4.14 above presents the proliferation of hFOB cells cultured on all scaffolds as determined by MTT assay. The cell numbers on all scaffolds increased significantly from 1 to 7 days but there is some reduction in cell numbers at day 3. In addition, the cell numbers on HPMC/PVA scaffolds incorporated with various amount of CNC increased obviously starting from day 3 to day 7 but no significant difference existed between them. However, the cell numbers on HPMC/PVA scaffolds exhibited only smaller significant increase from day 3 to day 7, respectively.

The quantitative analysis of DAPI staining of hFOB cells cultured on all scaffolds is shown in Figure 4.15. The results obtained from fluorescent microscope that detect nucleus cells indicate that more cells grew on the HPMC/PVA/CNC scaffolds than on HPMC/PVA scaffolds at each time point. Results exhibited that the incorporation of CNC up to 7 wt% into HPMC/PVA scaffolds did not present any inhibitory influence on the cytocompatibility characteristic of the HPMC/PVA scaffolds, however further addition of CNC up to 5 wt% reduced the cell viability. This result also shows how the CNC sheets provide a noncytotoxic environment for cells to remain viable, as cell metabolism was constant between 3 and 7 days for S-CNC aerogels (Daniel A. Osorio, 2019).



(a)

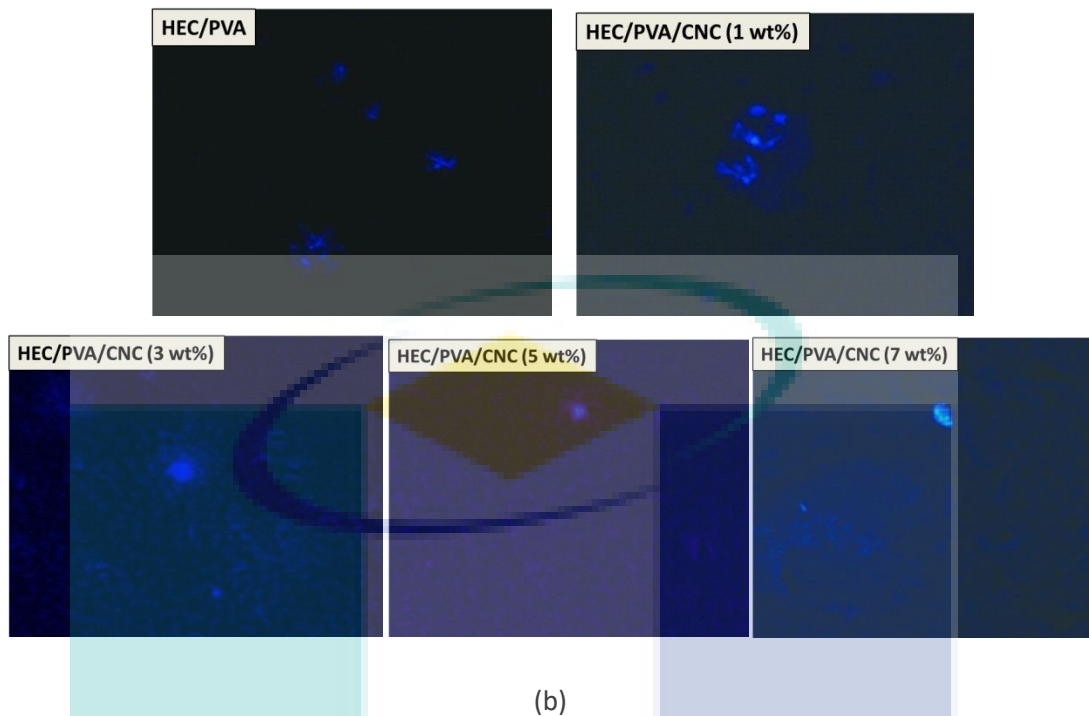
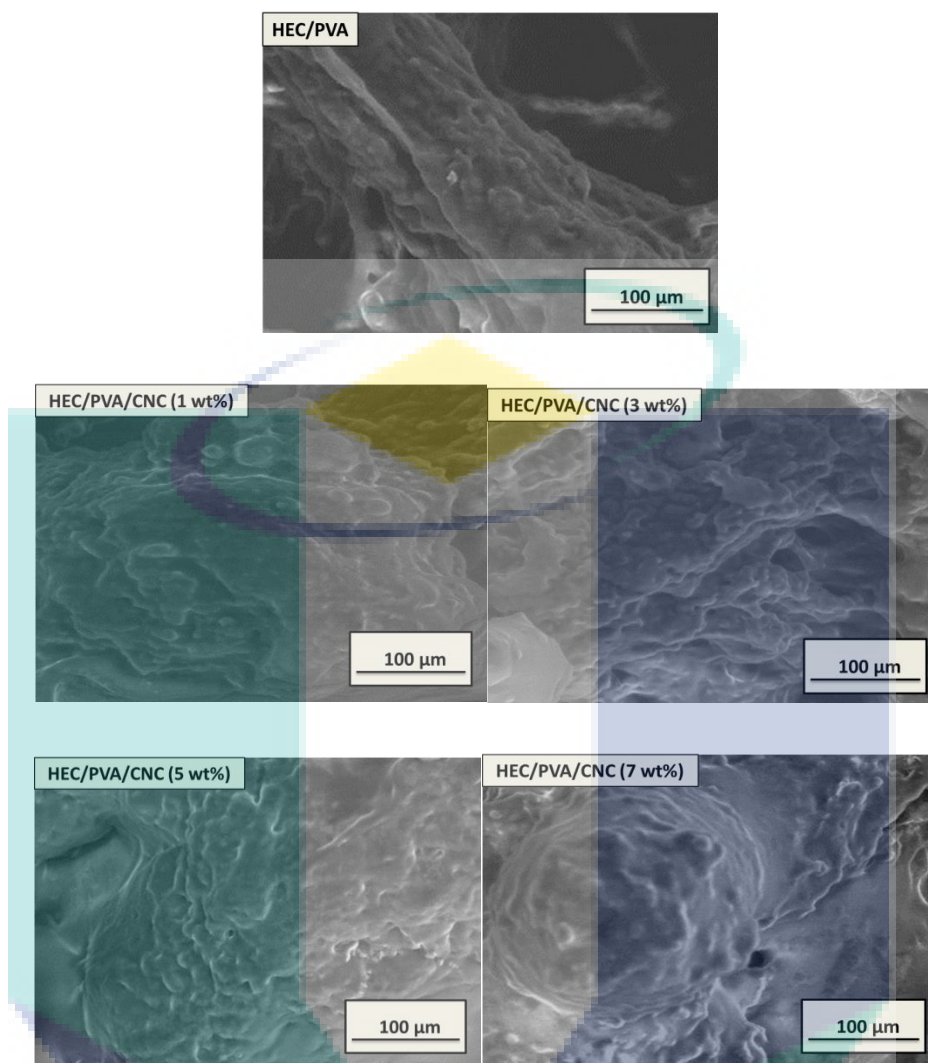


Figure 4.15 DAPI stained osteoblast cells grown in scaffolds at (a) 3 days and (b) 7 days

#### 4.4.2 hFOB cells morphology studies on scaffolds

hFOB cells cultured for 3 and 7 days on the samples were also observed by SEM. Figure 4.16 presents the SEM images of cells cultured on the samples at 3 and 7 days. Round shape morphology of osteoblast cells adhered on the surface of the all scaffolds. It is clearly observed that the cells exhibited slightly rough surface for all blended scaffolds. Incorporated scaffolds with CNC make the surface even rougher. After 3 days of cell culture, it was observed that cells get adhered to the scaffold and have polygonal morphology with the cell membrane being somewhat flattened onto the rough surface of the scaffold, created by HPMC/PVA/CNC particles.





(a)

UMP

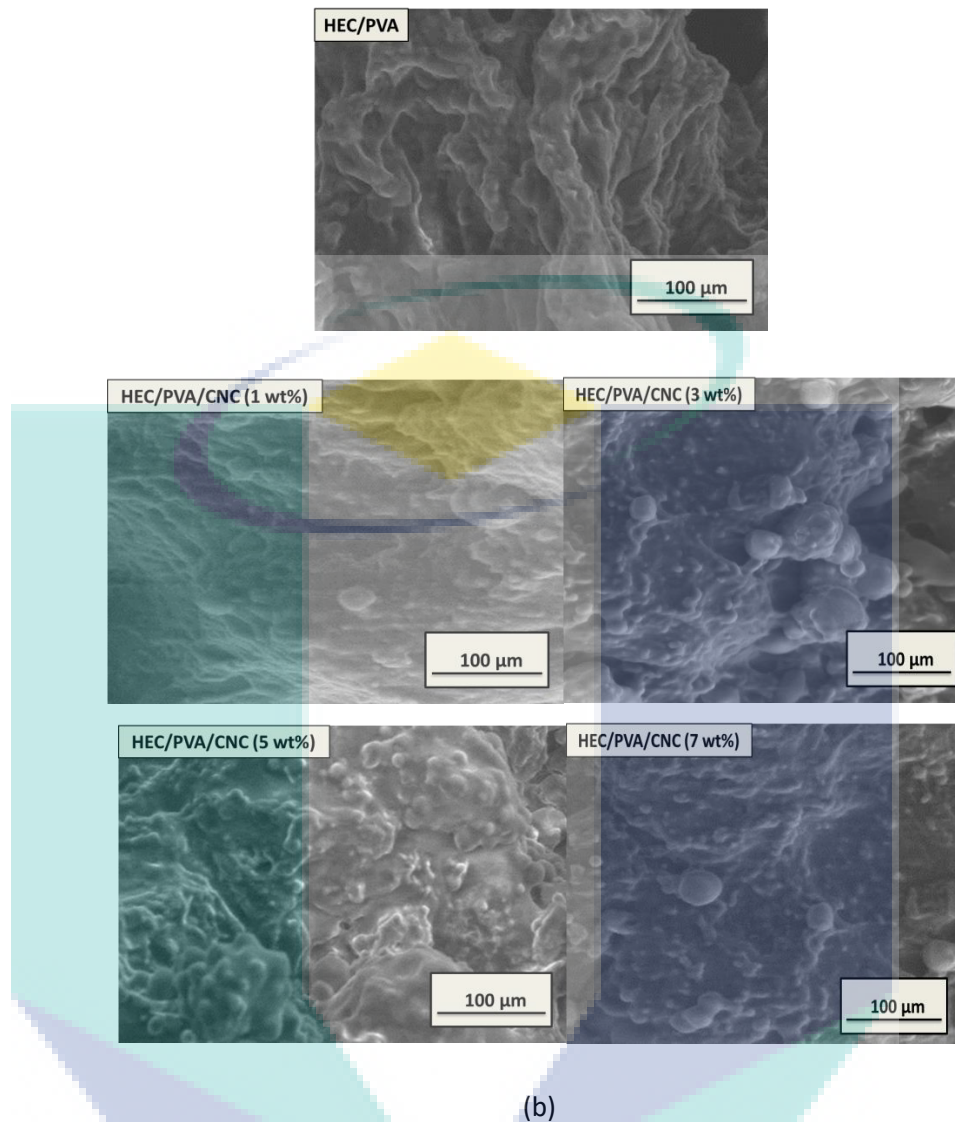
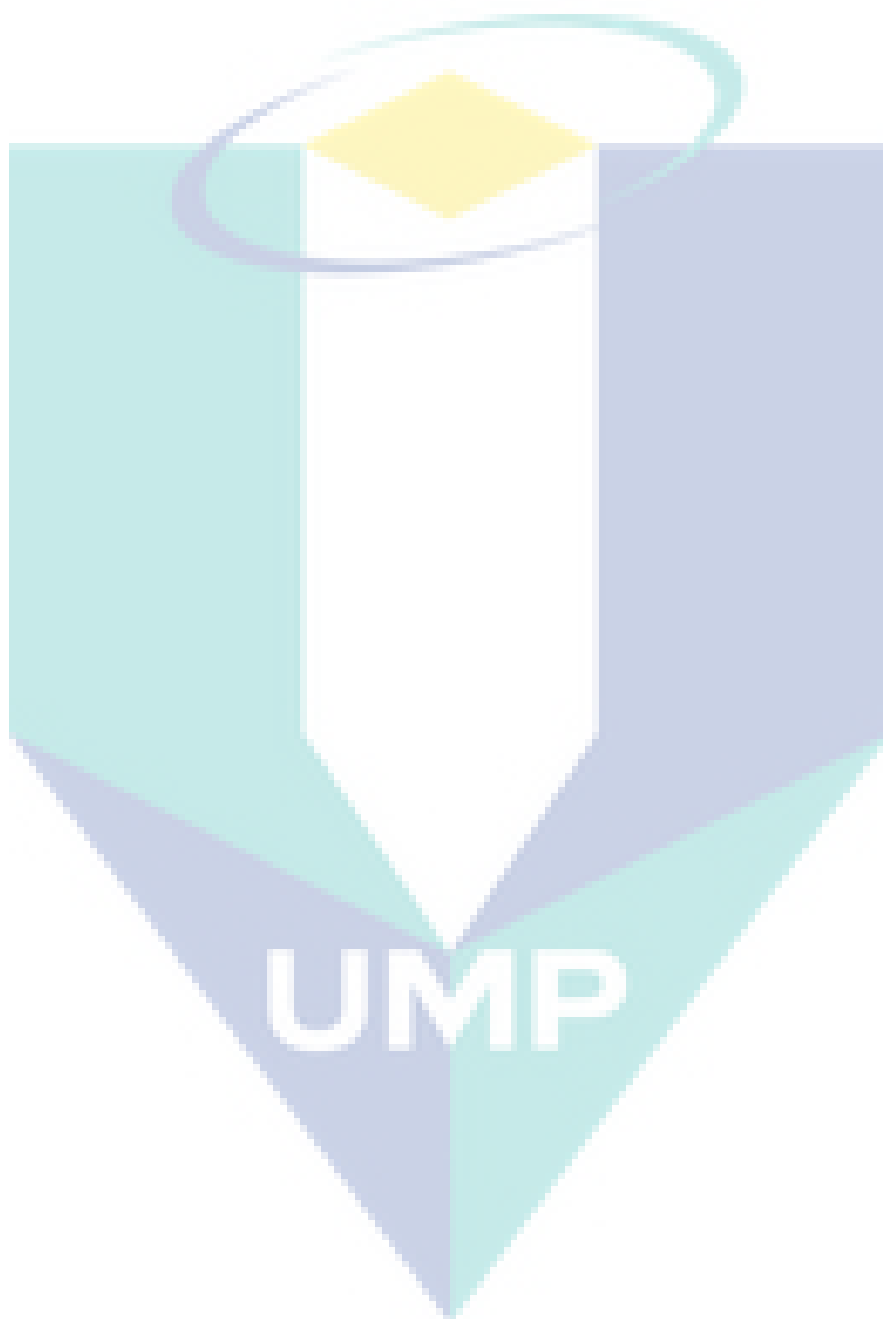


Figure 4.16 SEM micrograph images of hFOB cells attached on after (a) day 3 and (b) day 7 cell culture (black arrow indicates the growth cells)

At 7 days of cell culture, more flat osteoblast cells were produced indicating that the osteoblast cell proliferation had begun. SEM image of osteoblast cell-scaffolds depicts that osteoblast cells have spread all around the porous structure of the scaffold and covered almost the entire scaffold's surface at 7 days. The cells on the HPMC/PVA/CNC scaffolds spread better than on HPMC/PVA scaffolds as the incubation time increased. This result was also supported with MTT assay, which confirmed the potential of HPMC/PVA/CNC scaffold towards bone tissue regeneration.

All scaffolds showed low toxicity and supported the growth of hFOB cells. This observation will be further proven by the following statistics analysis of cellular

proliferation and viability of cell growth. Great cell attachment, adherence and proliferation are suitable remarks for in vivo culture.



## CHAPTER 5

### CONCLUSION

#### 5.1 Summary

To conclude, HPMC/PVA/CNCs demonstrates greater response towards hFOB cells with highest number of viable cells. All freeze-dried scaffolds show excellent cell attachment, adherence and proliferation, with more prominent results in HPMC/PVA/CNC (3 wt%). In this study, incorporated CNC indicating the great influence with HPMC/PVA blended for tissue engineering. Overall, all scaffolds endorse good biocompatibility, non-toxicity and could be potential substrates for skin tissue engineering.

The results demonstrated that the HPMC/PVA/CNC scaffold should be a promising candidate for proliferation, differentiation and mineralization of osteoblasts, and potentially can be used for bone tissue regeneration. These scaffolds can promote cells migration and stimulate cell proliferation and mineralization. Osteoblasts play an important role in the formation, growth, and repair of the bone, as they can form organic, non-mineralized bone matrix. Osteoblasts were found to be viable within all scaffolds suggesting that the environment could sustain osteoblast growth and proliferation.

#### 5.2 Recommendation for further research

1. There are several characterization testing could be conducted such as antimicrobial, XRD analysis, contact angle of samples to ensure its effectiveness.
2. The polymer solution and prepared freeze-dried porous scaffolds should be kept in dry cabinet to avoid any contamination occur such as fungal growth.

## REFERENCES

- Ali, M. E., & Lamprecht, A. (2017). Spray freeze drying as an alternative technique for lyophilization of polymeric and lipid-based nanoparticles. *Int J Pharm*, 516(1-2), 170-177.
- Bhat, S., & Kumar, A. (2013). Biomaterials and bioengineering tomorrow's healthcare. *Biomatter*, 3(3).
- Borkotoky, S. S., Dhar, P., & Katiyar, V. (2018). Biodegradable poly (lactic acid)/Cellulose nanocrystals (CNCs) composite microcellular foam: Effect of nanofillers on foam cellular morphology, thermal and wettability behavior. *Int J Biol Macromol*, 106, 433-446.
- Caló, E., & Khutoryanskiy, V. V. (2015). Biomedical applications of hydrogels: A review of patents and commercial products. *European Polymer Journal*, 65, 252-267.
- Clarke, B. (2008). Normal bone anatomy and physiology. *Clin J Am Soc Nephrol*, 3 Suppl 3, S131-139.
- Daniel A. Osorio, B. E. J. L., Jacek M. Kwiecien, Xiaoyue Wang, Iflah Shahid, Ariana L. Hurley, Emily D. Cranston, Kathryn Grandfield. (2019). Cross-linked Cellulose Nanocrystal Aerogels as Viable Bone Tissue Scaffolds.
- Edwards, J. V., Prevost, N., Sethumadhavan, K., Ullah, A., & Condon, B. (2013). Peptide conjugated cellulose nanocrystals with sensitive human neutrophil elastase sensor activity. *Cellulose*, 20(3), 1223-1235.
- Fonte, P., Reis, S., & Sarmiento, B. (2016). Facts and evidences on the lyophilization of polymeric nanoparticles for drug delivery. *J Control Release*, 225, 75-86.
- Gavasane, A. J. (2014). Synthetic Biodegradable Polymers Used in Controlled Drug Delivery System: An Overview. *Clinical Pharmacology & Biopharmaceutics*, 3(2).
- Gokmen, F. O., Rzayev, Z. M., Salimi, K., Bunyatova, U., Acar, S., Salamov, B., & Turk, M. (2015). Novel multifunctional colloidal carbohydrate nanofiber electrolytes with excellent conductivity and responses to bone cancer cells. *Carbohydr Polym*, 133, 624-636.

Hirano, Y., & Mooney, D. J. (2004). Peptide and Protein Presenting Materials for Tissue Engineering. *Advanced Materials*, 16(1), 17-25.

Kanimozhi, K., Khaleel Basha, S., & Sugantha Kumari, V. (2016). Processing and characterization of chitosan/PVA and methylcellulose porous scaffolds for tissue engineering. *Mater Sci Eng C Mater Biol Appl*, 61, 484-491.

Kasper, J. C., Winter, G., & Friess, W. (2013). Recent advances and further challenges in lyophilization. *Eur J Pharm Biopharm*, 85(2), 162-169.

Kneissel, J. A. G. a. M. (2017). *Bone Physiology and Biology*.

Kousaku Ohkawa, D. C., Hakyong Kim, Ayako Nishida, Hiroyuki Yamamoto<sup>1</sup>. (2004). Electrospinning of Chitosan. *Macromolecular Rapid Communications*, 1600-16005.

Kumar, A., Mandal, S., Barui, S., Vasireddi, R., Gbureck, U., Gelinsky, M., & Basu, B. (2016). Low temperature additive manufacturing of three dimensional scaffolds for bone-tissue engineering applications: Processing related challenges and property assessment. *Materials Science and Engineering: R: Reports*, 103, 1-39.

MacNeil, S. (2007). Progress and opportunities for tissue-engineered skin. *Nature*, 445(7130), 874-880.

Merrill, N. A. P. a. E. W. (1976). Differential Scanning Calorimetry of Crystallized PVA Hydrogels. *Journal of applied polymer science*, 20, 1457-1465.

Ng, H. M., Saidi, N. M., Omar, F. S., Ramesh, K., Ramesh, S., & Bashir, S. (2018). Thermogravimetric Analysis of Polymers. In *Encyclopedia of Polymer Science and Technology* (pp. 1-29).

Preethi Soundarya, S., Sanjay, V., Haritha Menon, A., Dhivya, S., & Selvamurugan, N. (2018). Effects of flavonoids incorporated biological macromolecules based scaffolds in bone tissue engineering. *Int J Biol Macromol*, 110, 74-87.

Saber-Samandari, S., Saber-Samandari, S., Kiyazar, S., Aghazadeh, J., & Sadeghi, A. (2016). In vitro evaluation for apatite-forming ability of cellulose-based nanocomposite scaffolds for bone tissue engineering. *Int J Biol Macromol*, 86, 434-442.

- Salehpour, S., Rafieian, F., Jonoobi, M., & Oksman, K. (2018). Effects of molding temperature, pressure and time on polyvinyl alcohol nanocomposites properties produced by freeze drying technique. *Industrial Crops and Products*, 121, 1-9.
- Shahbazarab, Z., Teimouri, A., Chermahini, A. N., & Azadi, M. (2018). Fabrication and characterization of nanobiocomposite scaffold of zein/chitosan/nanohydroxyapatite prepared by freeze-drying method for bone tissue engineering. *Int J Biol Macromol*, 108, 1017-1027.
- Tabuchi, R., Azuma, K., Izumi, R., Tanou, T., Okamoto, Y., Nagae, T., . . . Anraku, M. (2016). Biomaterials based on freeze dried surface-deacetylated chitin nanofibers reinforced with sulfobutyl ether beta-cyclodextrin gel in wound dressing applications. *Int J Pharm*, 511(2), 1080-1087.
- Ye, M., Mohanty, P., & Ghosh, G. (2014). Morphology and properties of poly vinyl alcohol (PVA) scaffolds: impact of process variables. *Mater Sci Eng C Mater Biol Appl*, 42, 289-294.
- Zhang, C., Salick, M. R., Cordie, T. M., Ellingham, T., Dan, Y., & Turng, L. S. (2015). Incorporation of poly(ethylene glycol) grafted cellulose nanocrystals in poly(lactic acid) electrospun nanocomposite fibers as potential scaffolds for bone tissue engineering. *Mater Sci Eng C Mater Biol Appl*, 49, 463-471.
- Zhang, H., Nie, H., Li, S., White, C. J. B., & Zhu, L. (2009). Crosslinking of electrospun polyacrylonitrile/hydroxypropyl methylcellulose composite nanofibers. *Materials Letters*, 63(13-14), 1199-1202.
- Zhou, X. H., Wei, D. X., Ye, H. M., Zhang, X., Meng, X., & Zhou, Q. (2016). Development of poly(vinyl alcohol) porous scaffold with high strength and well ciprofloxacin release efficiency. *Mater Sci Eng C Mater Biol Appl*, 67, 326-335.
- Zulkifli, F. H., Hussain, F. S., Rasad, M. S., & Mohd Yusoff, M. (2014). Nanostructured materials from hydroxypropyl methylcellulose for skin tissue engineering. *Carbohydr Polym*, 114, 238-245.